Optimization for the propagation of a multiparticle quantum walk in a one-dimensional lattice

Daer Feng [1,2,3] and Shengshi Pang [1,4,*]

[1] School of Physics, Sun Yat-Sen University, Guangzhou, Guangdong 510275, China
[2] Institute of Physics, Chinese Academy of Sciences, Beijing 100190, China
[3] School of Physical Sciences, University of Chinese Academy of Sciences, Beijing 100049, China
[4] Hefei National Laboratory, University of Science and Technology of China, Hefei 230088, China

(Received 8 February 2023; accepted 29 January 2024; published 1 May 2024)

The quantum walk is a quantum counterpart of the classical random walk that exhibits nonclassical behaviors and outperforms the classical random walk in various aspects. It has been known that a single particle can be propagated by a discrete-time quantum walk with a quadratic time scaling in the variance of position distribution, beating the linear time scaling in a classical random walk. In this paper, we consider the discrete-time quantum walk for multiple particles in a one-dimensional lattice, and investigate the optimization of the joint coin state to enhance the spatial propagation of the particles in the lattice. We study the asymptotic evolution of position distribution for multiple particles in the long-time limit, and analytically optimize the joint coin state to derive the maximum variance of the position distribution between the particles after the evolution of the quantum walk. An interesting result is that an optimized coin state always possesses specific exchange symmetry which can be characterized by a graph consisting of two disconnected complete subgraphs and the exchange symmetry can significantly influence the position correlations between the particles, showing the critical role of coin symmetry in the propagation of multiple particles by the quantum walk. We further study the entanglement of the optimized coin states to show the relation of the coin correlations to the particle position distribution.

DOI: 10.1103/PhysRevA.109.052402

I. INTRODUCTION

The quantum walk is an interesting quantum protocol with distinctive properties, such as quadratic speedup in the propagation of particles [1] and exponentially fast hitting [2,3], compared to its classical counterpart. These nonclassical behaviors have motivated intense research interest in exploring the intrinsic nature of the quantum walk and its potential applications [4,5]. So far, the quantum walk has been found to be a powerful tool in many quantum computing and quantum information tasks, e.g., spatial search [6–8], graph isomorphism testing [9–12], universal quantum computation [13–15], and quantum teleportation [16,17]. Quantum walks can also simulate physical phenomena in condensed matter physics such as Anderson localization and Bloch oscillations. Anderson localization [18], the absence of diffusion of a quantum mechanical state, can be produced in a quantum walk when the walk is subjected to disorder [19,20] or when the walk is inhomogeneous in the transition of a walker from one site to the others dependent on both the coin state and the position state [21,22]. The relation between the localization and the degeneracy of the eigenstates of a quantum walk is studied in Refs. [23,24]. Lin *et al.* simulated the non-Hermitian topological Anderson insulator experimentally by disordered photonic quantum walks [25].

Quantum walks have been realized experimentally in a vast variety of physical systems [26] such as superconducting qubits [27,28], optical lattices [29], photons [30–40], Bose-Einstein condensates [41,42], and trapped ions [43–46]. Experimental realizations of quantum walks via photons [47,48] and particularly the Hong-Ou-Mandel effect [49,50] exhibit different dynamics depending on the photon indistinguishability and statistics. Vertex search in graphs and graph isomorphism testing have been implemented on silicon photonic quantum walk processors [51].

Two types of formulations have been developed for quantum walks so far: the discrete-time quantum walk and the continuous-time quantum walk. The continuous-time quantum walk was proposed by Farhi and Gutmann as a powerful computational model that provides exponential speedup in penetrating a decision tree to outperform its classical counterpart [52]. The discrete-time quantum walk was introduced by Aharonov *et al.* [53], and it differs from the continuous-time quantum walk in that the walkers evolve with discrete time steps, and extra degrees of freedom, coins, are introduced to control the shift directions of the walkers at each step. The discrete-time quantum walk is also found useful in different quantum algorithms [54]. And it inspires many variations of quantum walk models: the coin-flip operator can be position dependent [55], leading to the quantum-walk-based search algorithms [6]; the walker can possess more than one coin and the coins can be entangled [56–58]; etc. Extension of quantum walks to higher-dimensional lattices [59,60], entangled particles [11,12], and interacting particles [11,12,61–64] have also been explored.

The introduction of coin degrees of freedom has a substantial influence on quantum walks, as the coins enlarge

*pangshsh@mail.sysu.edu.cn

 ©2024 American Physical Society

the dimension of the joint Hilbert space of the particles and can be entangled or interacting with each other, which gives more possibility and flexibility in various quantum tasks. For example, the presence of coins may enhance the distinguishing power of quantum walks on nonisomorphic graphs [12], the Grover coin can enable the quantum-walk-based search algorithm to reach the time complexity $O(\sqrt{N})$ for a database of size N [8] in analogy to the well-known Grover search algorithm [65,66], the coin symmetry can lead to different conditions for infinite hitting time [67–69], the correlations between two coins can develop spatial correlations between the walkers [70], and the conditional shift can generate entanglement between the coin and position degrees of freedom [71–73]. Moreover, Tregenna *et al.* have analytically investigated the general two-dimensional unitary coin operation for a single-particle quantum walk and showed the effect of the coin operation on the asymmetry of the walker position distribution [74]. The effect of decoherence in the coins of a quantum walk has also been studied, showing that decoherence could slow down the spatial spreading of the particles in a quantum walk and lead to approximately linear growth of the position distribution, which is typically a classical behavior [75].

A fascinating property of discrete-time quantum walks is that the variance of the position distribution of a single-particle quantum walk scales quadratically with time, compared to the linear time scaling of position variance in the classical random walk [54], implying a particle propagates much faster by quantum walk than by the classical counterpart, which is essentially rooted in the interference effect of different evolution paths in quantum walks [53,76]. And the coin state can tune the interference effect of the quantum walk and influence the position distribution of the particles [74]. In particular, Omar *et al.* [77] elucidate that for a two-particle discrete-time quantum walk, the exchange symmetry and entanglement of the joint coin states can significantly change the position correlations of the particles and, as a consequence, alter the average distance between the particles and the speed that the particles are propagated by the quantum walk.

As the fast propagation of particles is a prominent advantage of quantum walks over classical random walks and the coin states can change the position distribution of particles as reviewed above, we consider the following question in this paper to explore the limit of advantage that quantum walk can reach in propagating particles: For an arbitrary number of particles, what kind of joint coin state can maximize the relative distance between the particles in a quantum walk? We quantify the relative distance of multiple particles by the variance of the position distribution between the particles, and use the asymptotic analysis approach to study the evolution of a multiparticle discrete-time quantum walk in a one-dimensional lattice. The position variance between the particles is obtained asymptotically in the long-time limit, and the joint coin state is further analytically optimized to derive the maximum of position variance. An interesting result is that the optimized coin states always possess specific partial exchange symmetry between the particles and the symmetry can be characterized in a graphical approach. The entanglement and the two-particle correlations of the optimized coin states are also investigated in detail and illustrated by numerical computation.

The paper is structured as follows. In Sec. II, we provide preliminaries for the discrete-time quantum walk and the extension to the multiparticle case. Section III studies the evolution of multiparticle quantum walks for an arbitrary number of particles and obtains the asymptotic position variance between the particles to characterize the propagation property of multiparticle quantum walks. In Sec. IV, we apply the result of position variance to the case that the coins can be initially entangled and analytically optimize the coin state to derive the bounds of the position variance between the particles. Section V reveals the exchange symmetry of the optimized coin state and its crucial role in the position variance of the particles, and explores the entanglement and position correlations between the walkers. The paper is finally concluded in Sec. VI.

II. PRELIMINARIES

In this section, we introduce preliminaries of multiparticle discrete-time quantum walks and notations that will be used in this paper.

For discrete-time quantum walks in an infinite one-dimensional lattice, particles are located on discrete sites and possess coins to determine the shift directions of the particles at each time step. The Hilbert space of single-particle quantum walks in a one-dimensional lattice can be decomposed as $\mathscr{H} = \mathscr{H}_{\text{position}} \otimes \mathscr{H}_{\text{coin}}$, in which a single-particle state at position x with the coin upwards or downwards can be written as $|x\rangle \otimes |\uparrow\rangle$ or $|x\rangle \otimes |\downarrow\rangle$, respectively. The unitary evolution of the particle is given by

$$\hat{U} = \hat{S} \cdot (\hat{I} \otimes \hat{C}), \tag{1}$$

where $\hat{C}$ is a coin operator that flips the coin and $\hat{S}$ is the shift operator that changes the position of the particle dependent on its coin state. $\hat{S}$ usually takes the following form:

$$\hat{S} = \hat{Q} \otimes |\uparrow\rangle\langle\uparrow| + \hat{Q}^{\dagger} \otimes |\downarrow\rangle\langle\downarrow|, \tag{2}$$

where $\hat{Q}$ and $\hat{Q}^{\dagger}$ are the shift operators in the one-dimensional lattice. If $|x\rangle$ denotes the eigenstate of the position operator $\hat{x}$ with eigenvalue x, then $\hat{Q}$ and $\hat{Q}^{\dagger}$ can be chosen as

$$\hat{Q} = \sum_x |x+1\rangle\langle x|, \quad \hat{Q}^{\dagger} = \sum_x |x-1\rangle\langle x|. \tag{3}$$

To generalize the quantum walk in a one-dimensional lattice to noninteracting multiparticle cases, the evolution operator becomes the tensor product of single-particle evolution operators; i.e., $\hat{U}_n = \hat{U}^{\otimes n}$ for n particles. For an initial state as $|\psi_0\rangle$, the final state after t steps of evolution is $|\psi_t\rangle = \hat{U}_n^t|\psi_0\rangle$. A general n-particle initial state for a discrete-time quantum walk can be written as

$$|\psi_0\rangle = \sum a_{x_1s_1,\ldots,x_ns_n}|x_1s_1\rangle \otimes \cdots \otimes |x_ns_n\rangle. \tag{4}$$

Here $|x_i\rangle$ and $|s_i\rangle$ denote the eigenstates of the position operator $\hat{x}$ and the Pauli operator $\hat{\sigma}_z$ of the ith particle. After t steps of evolution, the final state of the particles can be obtained by calculating the linear combination of the evolved basis states, which are the tensor products of the final states of single-particle walks,

$$|\psi_t\rangle = \sum a_{x_1s_1,\ldots,x_ns_n}\hat{U}^t|x_1s_1\rangle \otimes \cdots \otimes \hat{U}^t|x_ns_n\rangle. \tag{5}$$

The quantum walk with two particles was studied in Ref. [77], and the exchange symmetry of the two particles was shown to have significant influence on the evolution. For more particles, Chandrashekar and Busch [78] considered the multiparticle quantum walk initialized in an uncorrelated state. When the particles are uncorrelated initially, the final state can be written as $\hat{U}^t|\phi_1\rangle \otimes \hat{U}^t|\phi_2\rangle \otimes \cdots \otimes \hat{U}^t|\phi_n\rangle$, where $|\phi_i\rangle$ is the initial single-particle state of the ith particle. But in this paper, we consider a more general situation in which the initial state is in the form of Eq. (4), which generally describes distinguishable particles but can also describe indistinguishable particles when it is invariant under arbitrary particle exchange.

The coin operator can be an arbitrary SU(2) transformation in general; i.e., regardless of a global phase,

$$\hat{C} = \begin{bmatrix} \sqrt{\rho} & \sqrt{1-\rho}e^{i\theta} \\ \sqrt{1-\rho}e^{i\varphi} & -\sqrt{\rho}e^{i(\varphi+\theta)} \end{bmatrix}, \tag{6}$$

where $0 \leqslant \rho \leqslant 1$ and $0 \leqslant \theta, \varphi \leqslant \pi$. In the current work, we choose the Hadamard operator to be the coin operator.

III. POSITION VARIANCE OF THE MULTIPARTICLE QUANTUM WALK

In this section, we define the position variance between particles and calculate the position variance of a general n-particle state for a sufficiently large number of walk steps.

In a classical multiparticle random walk, the variance of the position distribution between the particles grows linearly with the number of time steps, as is proven in Appendix 1. In this paper, we first show that for a general multiparticle quantum walk, the position variance can grow quadratically with the number of time steps, which also holds true when the particles are initially entangled and the different walk paths may interfere [76].

The variance of the position distribution between particles is defined as

$$\hat{D} = \sum_i \left[\hat{x}_i - \frac{1}{n}\sum_j \hat{x}_j\right]^2, \tag{7}$$

where $\hat{x}_i$ represents the position of the ith particle, and $\hat{D}$ can be decomposed into two parts,

$$\hat{D} = \frac{n-1}{n}\sum_i \hat{x}_i^2 - \frac{1}{n}\sum_{j\neq j'} \hat{x}_j\hat{x}_{j'}, \tag{8}$$

consisting of single-particle operators and two-particle operators. Note that this definition considers only the position variance *between* the particles, excluding the position variance of each single particle which is studied in Refs. [1,54,79] and also scales quadratically with time. When $n = 2$, the variance $\hat{D}$ can be reduced to the squared distance between the two particles in Ref. [77].

A. Diagonalization of the evolution operator

Diagonalizing the evolution operator of the particles will help simplify the calculation of the evolution. Following the idea of discrete-time Fourier transform for quantum walks [75,79], one can transform the state of the particles from the position space into the momentum space, and the transformation between the two spaces is given by

$$|K\rangle = \frac{1}{\sqrt{2\pi}}\sum_x e^{iKx}|x\rangle, \tag{9}$$

where $|K\rangle$ and $|x\rangle$ are the basis states of the momentum space and the position space, respectively. It can be verified that $|K\rangle$ preserves the orthonormality $\langle K'|K\rangle = \delta(K'-K)$ and is the eigenstate of $\hat{Q}$ with eigenvalue e^{-iK} and the eigenstate of $\hat{Q}^\dagger$ with eigenvalue e^{iK}; therefore, applying the conditional shift $\hat{S}$ given in Eq. (2) to $|K\rangle$ merely induces extra phases in the coin space, and the evolution $\hat{U}$ of the particles in the joint Hilbert space of the position and coin can be factorized as

$$\hat{U} = \int_{-\pi}^{\pi} dK|K\rangle\langle K| \otimes \hat{U}_K, \tag{10}$$

where $\hat{U}_K = (e^{-iK}|\uparrow\rangle\langle\uparrow| + e^{iK}|\downarrow\rangle\langle\downarrow|)\hat{C}$ is the conditional evolution in the coin space with a given momentum K. If we choose the coin-flip operator to be the Hadamard operator

$$\hat{H} = \frac{1}{\sqrt{2}}(|\uparrow\rangle\langle\uparrow| + |\uparrow\rangle\langle\downarrow| + |\downarrow\rangle\langle\uparrow| - |\downarrow\rangle\langle\downarrow|), \tag{11}$$

then $\hat{U}_K$ can be written as

$$\hat{U}_K = \frac{e^{-iK}}{\sqrt{2}}(|\uparrow\rangle\langle\uparrow| + |\uparrow\rangle\langle\downarrow|) + \frac{e^{iK}}{\sqrt{2}}(|\downarrow\rangle\langle\uparrow| - |\downarrow\rangle\langle\downarrow|). \tag{12}$$

Further diagonalization of the evolution $\hat{U}_K$ gives the eigenstates as

$$\begin{aligned} |d_1(K)\rangle &= -\frac{e^{-iK}}{\sqrt{2N(K)}}|\uparrow\rangle + \frac{1}{\sqrt{2N(\pi-K)}}|\downarrow\rangle, \\ |d_2(K)\rangle &= \frac{e^{-iK}}{\sqrt{2N(\pi-K)}}|\uparrow\rangle + \frac{1}{\sqrt{2N(K)}}|\downarrow\rangle, \end{aligned} \tag{13}$$

with λ_j $(j = 1, 2)$ as the corresponding eigenvalues,

$$\lambda_j(K) = (-1)^j\frac{1}{2}\sqrt{3+\cos(2K)} - \frac{i\sin(K)}{\sqrt{2}}, \tag{14}$$

where $N(K) = (1+\cos^2 K) + \cos K\sqrt{1+\cos^2 K}$.

Finally, we arrive at the diagonalized representation of the momentum-dependent unitary evolution $\hat{U}_K$ in Eq. (10),

$$\hat{U}_K = \lambda_1|d_1(K)\rangle\langle d_1(K)| + \lambda_2|d_2(K)\rangle\langle d_2(K)|. \tag{15}$$

B. Average position variance of the multiparticle walk

As calculating the exact position variance between particles is generally complex, we will focus on the case for a sufficiently large number of time steps in this paper. We outline the method to compute the asymptotic variance below, and leave the details of derivation to Appendix 3.

For a general n-particle quantum walk with initial state given in Eq. (4), the average position variance of the particles after t steps of evolution is $\langle\psi_0|(\hat{U}_n^\dagger)^t\hat{D}\hat{U}_n^t|\psi_0\rangle$, and it can be broken down into the summation of the terms in the following form:

$$\begin{aligned}&\langle x_1's_1'|\cdots\langle x_n's_n'|(\hat{U}_n^\dagger)^t\hat{D}\hat{U}_n^t|x_1s_1\rangle\cdots|x_ns_n\rangle\\&=\frac{n-1}{n}\sum_i\langle x_i's_i'|(\hat{U}^\dagger)^t\hat{x}_i^2\hat{U}^t|x_is_i\rangle\prod_{\gamma=1,\gamma\neq i}^n\delta_{x_\gamma's_\gamma',x_\gamma s_\gamma}\\&\quad-\frac{1}{n}\sum_{j\neq k}\langle x_j's_j'|(\hat{U}^\dagger)^t\hat{x}_j\hat{U}^t|x_js_j\rangle\langle x_k's_k'|(\hat{U}^\dagger)^t\hat{x}_k\hat{U}^t|x_ks_k\rangle\\&\quad\times\prod_{\gamma=1,\gamma\neq j,k}^n\delta_{x_\gamma's_\gamma',x_\gamma s_\gamma}.\end{aligned}\tag{16}$$

$\delta_{x_\gamma's_\gamma',x_\gamma s_\gamma}$ is 1 when $x_\gamma'=x_\gamma$, $s_\gamma'=s_\gamma$ and 0 otherwise, implying the summands in the second line can contribute to the position variance only when the states of the particles other than the ith particle in the bra $\langle x_1's_1'|\cdots\langle x_n's_n'|$ and the ket $|x_1s_1\rangle\cdots|x_ns_n\rangle$ match. And a similar constraint applies to the summands in the third and fourth lines. For the matrix element $\langle x_i's_i'|(\hat{U}^\dagger)^t\hat{x}_i^2\hat{U}^t|x_is_i\rangle$, by the completeness of the basis $\{|K\rangle\otimes|d\rangle\}$ and noting that Eqs. (10) and (15) give the spectral decomposition of the evolution operator, we can obtain

$$\begin{aligned}&\langle x_i's_i'|(\hat{U}^\dagger)^t\hat{x}_i^2\hat{U}^t|x_is_i\rangle\\&=\int_{-\pi}^{\pi}\int_{-\pi}^{\pi}\mathrm{d}K'\mathrm{d}K\sum_{d,d'}\langle x_i's_i'|K'd'\rangle\\&\quad\times\langle K'd'|(\hat{U}^\dagger)^t\hat{x}_i^2\hat{U}^t|Kd\rangle\langle Kd|x_is_i\rangle\\&=\int_{-\pi}^{\pi}\int_{-\pi}^{\pi}\mathrm{d}K'\mathrm{d}K\sum_{d,d'}\\&\quad\times\langle x_i'|K'\rangle\langle s_i'|d'\rangle\langle K|x_i\rangle\langle d|s_i\rangle\langle d'|(\hat{U}_{K'}^\dagger)^t|d'\rangle\\&\quad\times\langle K'|\hat{x}_i^2|K\rangle\langle d'|d\rangle\langle d|\hat{U}_K^t|d\rangle.\end{aligned}\tag{17}$$

Representing $\hat{x}^2$ in the momentum space produces the periodic extension of the derivative of the Dirac delta function with period 2π,

$$\begin{aligned}\langle K'|\hat{x}_i^2|K\rangle&=\sum_{x=-\infty}^{\infty}\langle K'|\hat{x}_i^2|x\rangle\langle x|K\rangle\\&=-\sum_{l=-\infty}^{\infty}\delta^{(2)}(K'-K+2\pi l),\end{aligned}\tag{18}$$

where $l\in\mathbb{Z}$. So, the matrix elements of $(\hat{U}^\dagger)^t\hat{x}_i^2\hat{U}^t$ can be simplified to

$$\begin{aligned}&\langle x_i's_i'|(\hat{U}^\dagger)^t\hat{x}_i^2\hat{U}^t|x_is_i\rangle\\&=-\frac{1}{2\pi}\int_{-\pi}^{\pi}\int_{-\pi}^{\pi}\mathrm{d}K'\mathrm{d}K\sum_{d,d'}e^{iK'x_i'}e^{-iKx_i}\langle s_i'|d'\rangle\langle d|s_i\rangle\\&\quad\times\langle d'|(\hat{U}_{K'}^\dagger)^t|d'\rangle\delta^{(2)}(K'-K)\langle d'|d\rangle\langle d|\hat{U}_K^t|d\rangle\\&=-\frac{1}{2\pi}[t^2I_{A2}(x_i'-x_i,s_i',s_i)+tI_{A1}(x_i',x_i,s_i',s_i)\\&\quad+I_{AC}(x_i',x_i,s_i',s_i)+I_{Ao}(x_i',x_i,s_i',s_i;t)].\end{aligned}\tag{19}$$

Similarly,

$$\begin{aligned}&\langle x_j's_j'|(\hat{U}^\dagger)^t\hat{x}_j\hat{U}^t|x_js_j\rangle\\&=-\frac{i}{2\pi}[tI_B(x_j'-x_j,s_j',s_j)+I_{B_1}(x_j',x_j,s_j',s_j)\\&\quad+I_{Bo}(x_j',x_j,s_j',s_j;t)].\end{aligned}\tag{20}$$

In the above equations, I_{A2}, I_{A1}, I_{AC}, I_B, and I_{B_1} are coefficients for different powers of t and can be calculated using the residue theorem. The integrals in the term t^2 of the position variance are

$$I_{A2}(x,s',s)=\begin{cases}(1-\sqrt{2})f(0), & x=0,s'=s\\ f(x), & x\neq 0,s'=s\\ 0, & s'\neq s,\end{cases}\tag{21}$$

$$I_B(x,s',s)=\begin{cases}(-1)^s iI_{A2}(x,s',s), & s'=s\\ \frac{i}{2}[f(x)+f(x-(-1)^s\times 2)], & s'\neq s,\end{cases}\tag{22}$$

where $f(x)=\sqrt{2}\pi(\sqrt{2}-1)^{|x|}\cos(\pi x/2)$. When s is $\uparrow$, it denotes the number 1, and $\downarrow$ denotes 0; i.e., when $s=\downarrow$, $(-1)^s=1$. The detailed expressions of integrals I_{A1}, I_{B_1}, I_{AC}, I_{Ao}, and I_{Bo} are given in Appendix 3.

I_{Ao} and I_{Bo} are integrals involving rapidly time-varying phases when t is large, which can be calculated by the stationary phase approximation [80]. The matrix elements (19) and (20) are the functions of the states $|x_is_i\rangle$ and $|x_i's_i'\rangle$ as well as the number of time steps, t, with the highest order of t being t^2. After a long time evolution, the t^2 term becomes dominant, so the other lower-order terms can be dropped. By plugging Eqs. (19) and (20) into Eq. (16) and summing up all the terms in the form of Eq. (16), it yields the average position variance for a given initial state in Eq. (4).

IV. BOUNDS OF POSITION VARIANCE

Now we consider the case in which the particles are initially uncorrelated in the spatial lattice but entangled in the coin space. We are concerned with how the position variance between the particles is dependent on the initial coin state, and we obtain the upper and lower bounds of the position variance when the number of time steps is large.

To simplify the representation of the coin state, we denote the basis states of the coin space, $|\uparrow\rangle$ and $|\downarrow\rangle$ as $|1\rangle$ and $|0\rangle$ and the coin state of the ith particle as $|s_i\rangle$. The combination of the coin states of all particles can be treated as a binary number and can be simply denoted by its numerical value, i.e., $|s_1s_2\cdots s_n\rangle=|2^{n-1}\times s_1+2^{n-2}\times s_2+\cdots+2s_{n-1}+s_n\rangle=|\xi\rangle$, where ξ is the numerical value of the binary number $s_1s_2\cdots s_n$. We assume the spatial state of the particles to be a product state, and the initial state can be written as

$$|\Psi\rangle=|x_1\rangle|x_2\rangle\cdots|x_n\rangle\otimes\sum_{\xi=0}^{2^n-1}a_\xi|\xi\rangle.\tag{23}$$

For simplicity, we assume the particles to be located in the same arbitrary position for the rest of this paper.

The position variance $\langle\Psi|(\hat{U}^\dagger)^t\hat{D}\hat{U}^t|\Psi\rangle$ after t steps of evolution is generally complicated, but can be expanded to a power series of t. For a large t, the t^2 term dominates

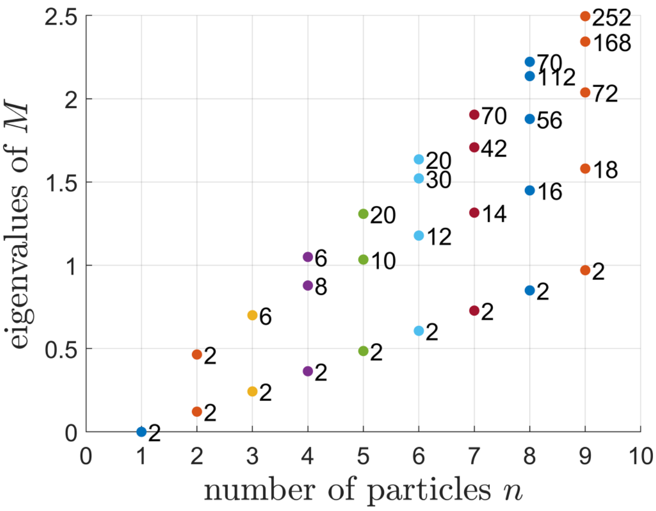

FIG. 1. Distribution of the eigenvalues of matrix M in Eq. (25). The eigenvalues are the extremized coefficients of the leading time-quadratic term in the position variance, for different numbers of particles. The numbers next to the points denote the degrees of degeneracy of the eigenvalues.

the variance, so we will mainly consider the coefficient of t^2 denoted as c_2 in the following. It can be verified that c_2 has a quadratic form of $a_0, a_1, \dots, a_{2^n-1}$ and their complex conjugates, which can be rearranged in the following matrix form:

$$c_2 = [a_0^*, a_1^*, \dots, a_{2^n-1}^*] M [a_0, a_1, \dots, a_{2^n-1}]^T, \tag{24}$$

where M collects all the coefficients of $a_i^* a_j$ in c_2. And it turns out that c_2 is independent of the initial positions of particles in the state $|\Psi\rangle$ in Eq. (23). The matrix M is obtained in Appendix 4, and the elements of M are obtained as

$$\begin{aligned} M_{ii} &= (n-1)(1-1/\sqrt{2}) \\ &\quad + \frac{1}{n}[n-(2W(i)-n)^2](1-1/\sqrt{2})^2, \\ M_{jk} &= \frac{2}{n}(1-1/\sqrt{2})^2[\delta_{d(j,k),1}(n-1 \\ &\quad - 2\min\{W(j),W(k)\}) - \delta_{d(j,k),2}], \end{aligned} \tag{25}$$

where $i, j, k \in \{0, 1, 2, \dots, 2^n - 1\}$, $j \neq k$, $W(i)$ is the Hamming weight of the binary representation of integer i, $d(j,k)$ is the Hamming distance between integers j and k, i.e., the number of bit positions where k differs from j, and δ is the Kronecker delta function.

The maximum and minimum values of c_2 are exactly the maximum and minimum eigenvalues of the matrix M since the complex vector $[a_0, a_1, \dots, a_{2^n-1}]$ is normalized, and the normalized eigenvectors of the matrix M are the extremal points for the coefficient c_2 [Eq. (24)] and equivalently for the quadratic term of t in the position variance of $|\Psi\rangle$. By numerical computation, the relation of the number of particles to the eigenvalues of M and their degeneracies is illustrated in Fig. 1. And it is proven in Appendix 5 that the eigenvalues are

$$\eta_k = \left(1-\frac{1}{\sqrt{2}}\right)^2 \left[\frac{8W(k)(n-W(k))}{n} + (n-1)\sqrt{2}\right], \tag{26}$$

where $k = 0, 2, \dots, 2^n - 2$. It can be inferred that $0 \leqslant W(k) \leqslant n-1, W(k) \in \mathbb{Z}$, and there are $C_{n-1}^{W(k)}$ different values of k's that correspond to the same value of $W(k)$. Note that for different values of k's, e.g., k and k', η_k and $\eta_{k'}$ take the same value when $W(k) = n - W(k')$, which should be taken into account in counting the degeneracies of the eigenvalues. The degeneracy of η_k is

$$\text{count}(\eta_k) = \begin{cases} 2, & k = 0 \\ 2(C_{n-1}^{W(k)} + C_{n-1}^{n-W(k)}), & k \neq 0, n \text{ is odd} \\ 2(C_{n-1}^{W(k)} + C_{n-1}^{n-W(k)}), & k \neq 0, W(k) \neq \frac{n}{2}, n \text{ is even} \\ 2C_{n-1}^{W(k)}, & W(k) = \frac{n}{2}, n \text{ is even.} \end{cases} \tag{27}$$

The calculation of the degeneracy of eigenvalues is also given in Appendix 5.

The eigenvectors for η_k turn out to be the kth and $(k+1)$th columns of matrix P, and P is a $2^n \times 2^n$ matrix consisting of 2×2 submatrices

$$P_{ik} = (-1)^{c(i,k)} Z^{d(i,k)} = (-1)^{c(i,k)} \begin{bmatrix} 0 & 1 \\ 1 & 2 \end{bmatrix}^{d(i,k)}, \tag{28}$$

where $i, k \in \{0, 2, \dots, 2^n - 2\}$ are the row and column locations of the upper left corner element of the submatrix P_{ik} in the matrix P. $c(i,k)$ denotes the number of bits on which the binary form of i and k have a common 1. The matrix P diagonalizes the matrix M by $P^{-1}MP$. For instance, when $n = 2$,

$$P = \left[\begin{array}{cc|cc} \overbrace{1 \quad 0}^{P_{00}} & & \overbrace{0 \quad 1}^{P_{02}} & \\ 0 & 1 & 1 & 2 \\ \hline 0 & 1 & -1 & 0 \\ \underbrace{1 \quad 2}_{P_{20}} & & \underbrace{0 \quad -1}_{P_{22}} & \end{array}\right]. \tag{29}$$

Then $P^{-1}MP = \text{diag}(\eta_0, \eta_0, \eta_2, \eta_2) = \text{diag}(\frac{3}{\sqrt{2}} - 2, \frac{3}{\sqrt{2}} - 2, 4 - \frac{5}{\sqrt{2}}, 4 - \frac{5}{\sqrt{2}})$.

By assigning the elements of column vectors in P after normalization to the corresponding coefficients a_ξ, we obtain optimized coin states $\sum_{\xi=0}^{2^n-1} a_\xi |\xi\rangle$.

The eigenvalues of the matrix M give the range of c_2, $\eta_{\min} \leqslant c_2 \leqslant \eta_{\max}$. According to Eq. (26), the largest eigenvalue for a given number of particles n is

$$\eta_{\max}(n) = \begin{cases} \left(1-\frac{1}{\sqrt{2}}\right)^2[(n-1)\sqrt{2} + 2n], & n \text{ even} \\ \left(1-\frac{1}{\sqrt{2}}\right)^2\left[(n-1)\sqrt{2} + 2n - \frac{2}{n}\right], & n \text{ odd,} \end{cases} \tag{30}$$

while the smallest eigenvalue is

$$\eta_{\min}(n) = \left(1-\frac{1}{\sqrt{2}}\right)^2 \sqrt{2}(n-1). \tag{31}$$

The eigenvalues $\eta_{\max}(n)$ and $\eta_{\min}(n)$ are positive, so both the upper bound and lower bound of the position variance grow quadratically with the number of time steps, t. The eigenvectors for $\eta_{\min}(n)$ are the columns $k = 0$ and $k = 1$ of the matrix P. And when n is odd, the eigenvectors for $\eta_{\max}(n)$ are the columns k and $k + 1$ where k satisfies $W(k) = \lceil n/2 \rceil$ or $W(k) = \lfloor n/2 \rfloor$; when n is even, the eigenvectors for $\eta_{\max}(n)$ are the columns k and $k + 1$ where k satisfies $W(k) = n/2$.

The above solution to the eigenvalue problem of the matrix M in the quadratic form of c_2 provides the optimized initial coin states and the extremal values for the leading term of t in the position variance of the n-particle state. For simplicity, we refer to these optimized coin states as eigenstates, and sometimes we refer to an eigenstate as the initial particle state combining both the optimized coin state and the positional state as is shown in Eq. (23).

V. SYMMETRY AND ENTANGLEMENT OF OPTIMIZED COIN STATES

Next, we proceed to study the relation between the extremal values of the coefficient c_2 for the quadratic term of t in the particle position variance and the symmetry of the initial coin states of the n particles. As we will see later, each eigenstate is invariant after arbitrary permutation among a subset of the particles. We define this invariance of the eigenstates as *partial exchange symmetry*.

A. Partial exchange symmetry of optimized coin states

In Eq. (23), the positional state is an arbitrary product state to make the results general, but it has been shown above that the initial positions of the particles do not affect the leading term $c_2 t^2$ in the variance of the particle positions. For convenience, we assume all of the particles to be located at the original point initially, so that the symmetry of the particles is only determined by the joint coin state. If we visualize the partial exchange symmetry of an eigenstate by assigning the particles to the vertices of an undirected graph and connecting a pair of particles with an edge if the state is unchanged after swapping those two particles, it turns out that the graph may be composed of two disconnected but complete subgraphs. This is illustrated in Fig. 2, and proven in Appendix 6.

It is shown that the number of possible ways p_k to exchange two particles that preserve an eigenstate is related to the eigenvalue η_k by $\eta_k = (1 - 1/\sqrt{2})^2[8(C_n^2 - p_k)/n + (n-1)\sqrt{2}]$, so one can deduce that the larger the p_k is, the smaller the eigenvalue η_k will be, and thus a greater degree of partial exchange symmetry of the eigenstate results in a smaller relative spreading distance of the quantum walk, which is essentially induced by a greater extent of constructive interference between the walking routes of the particles and more particles oriented in the same direction and thus closer to each other.

It can be proven that (see Appendix 6) if one denotes $n_\uparrow$ and $n_\downarrow$ as the numbers of "ones" and "zeros" in the binary form of k (k is even), respectively, then $p_k = \frac{n_\uparrow(n_\uparrow - 1)}{2} + \frac{n_\downarrow(n_\downarrow - 1)}{2}$, $n_\uparrow + n_\downarrow = n$, and the two disconnected subgraphs have $n_\uparrow$ and $n_\downarrow$ vertices, respectively. When $k = 0$, all the n particles are assigned to the same subgraph (actually the whole graph is connected in this case), which corresponds to the largest p_k

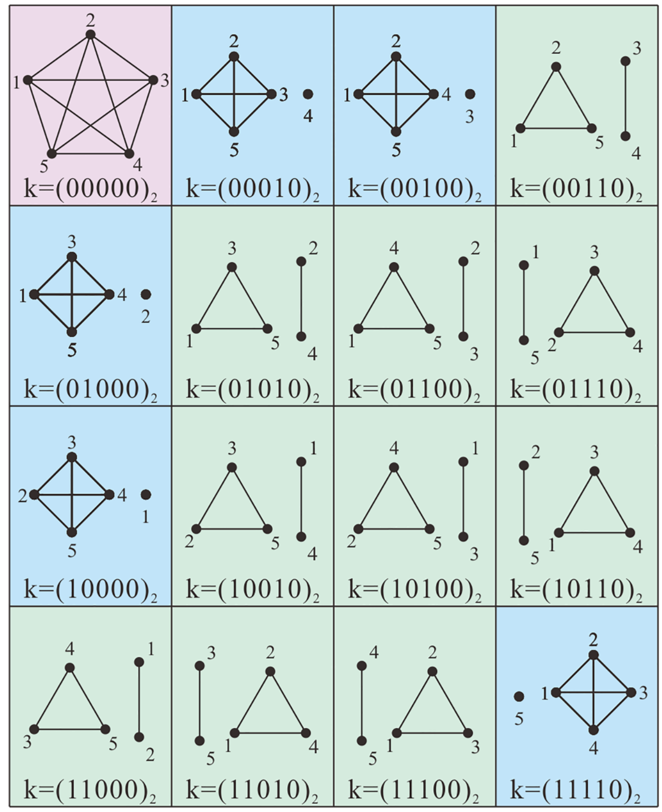

FIG. 2. Vertex partitions for eigenstates of $n = 5$ particles. The numbers near the vertices label different particles, and the subset that the ith particle belongs to depends on the ith bit of k. From left to right and then top to bottom, each cell of the table represents complete graph(s) corresponding to a different even number k ranging from 0 to $2^n - 2$, respectively, where k is the column subscript of the corresponding eigenvector in the matrix P. When k is odd, the vertex partition is the same as that of $k - 1$. Different background colors of the cells are assigned to the graphs with different structures, which also indicate different eigenvalues.

and the smallest η_k. The particles are closest to each other in this case and the eigenstate possesses the greatest exchange symmetry. When the particles are distributed as uniformly as possible between the two subgraphs, we obtain the smallest p_k and the particles turn out to be the most distant. Note there is no antisymmetric eigenstate here when $n > 2$ since the coin space of each particle is only two dimensional, in contrast to the case of two particles where both symmetric and antisymmetric coin states can exist but lead to drastically different position distributions [77].

It is worth noting that the framework of multiparticle quantum walks starts with distinguishable particles in this paper, but the above optimization results can actually also apply to indistinguishable or partially indistinguishable particles. While the nature of indistinguishable particles is intrinsically different from that of distinguishable particles, the states of fully or partially indistinguishable particles can be equivalently represented by fully or partially symmetric states of distinguishable particles. So in mathematics, the quantum walk of multiple indistinguishable particles can also be included in the current framework with proper symmetric multiparticle states. The above optimization of multiparticle position variance further implies that the states of distinguishable particles possess full or partial symmetry when the position variance is extremized, so the optimized states of distinguishable particles coincide with the states of fully or partially indistinguishable particles and the optimization results can thus be applicable to indistinguishable particles as well.

It should be clarified that the bipartite structures of the graphs in Fig. 2 do not mean that the two parts of the graph are not correlated. For the eigenstate associated with the kth eigenvector, if $k \neq 0$, the entanglement between the two disconnected parts of the graph can be quantified by the von Neumann entropy

$$S(\rho_\uparrow) = -\sum_{i=1,2} \nu_i \log \nu_i, \tag{32}$$

in which $\nu_1 = [1 + (3 - 2\sqrt{2})^{n-2}]^{-1}$ and $\nu_2 = [1 + (3 + 2\sqrt{2})^{n-2}]^{-1}$ for an even k, and $\nu_1 = [1 + (3 - 2\sqrt{2})^{n}]^{-1}$ and $\nu_2 = [1 + (3 + 2\sqrt{2})^{n}]^{-1}$ for an odd k (Appendix 7). $\rho_\uparrow$ denotes the reduced density matrix of the particles associated with $n_\uparrow$. Interestingly, the results of ν_1 and ν_2 rely on the parity of k only, independent of the specific value of k when k is restricted to be odd or even ($k \neq 0$). As $S(\rho_\uparrow)$ is nonzero, the two disconnected parts of the graphs are generally entangled for the variance of the particle positions to reach extremal values.

B. Dynamics of optimized coin states

Before concluding this paper, we try to dig a bit deeper into the dynamics of the particles in the two subgraphs. The initial positions of all particles are assumed to be zero.

For the case of $n = 7$, the average of $\hat{x}_i^2$ and two-particle position correlations of the eigenstate given by the column $k = (1001010)_2$ of the matrix P after an evolution of $t = 30$ steps are shown in Fig. 3. They are essentially the components of the position variance operator in Eq. (8). It can be seen that the particles in the same subgraph possess the same average value of $\hat{x}_i^2$ and the same particle position correlation due to the partial exchange symmetry and the evolution does not break this symmetry. The position correlations of two particles are positive if the particles are from the same subgraph and negative if from different subgraphs, because the particles from the two subgraphs are initially placed at the original point but oriented in different directions by their coins. The two-particle position correlations always remain the same if either particle is replaced by another particle in the same subgraph, since picking different particles from the same subgraph does not make any difference due to the partial exchange symmetry.

A more insightful observation of the position distribution of the particles is presented in Fig. 4. Particles in the same subgraph are more likely to be close to each other. But particles from different subgraphs, such as particles 1 and 2, are more distant. As is shown in Fig. 4(a), particle 1 is more likely to be found in negative positions while particle 2 is more likely to be found in positive positions, because we can see from the reduced density matrices of the initial coin state that the coins are on average oriented in the opposite directions. As a comparison, Fig. 4(b) illustrates the position distributions of

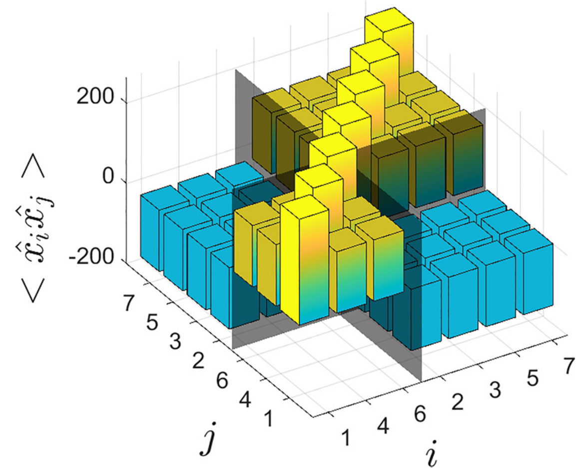

FIG. 3. Two-particle position correlations of the evolved eigenstate with $k = (1001010)_2, n = 7, t = 30$. i and j label the ith and jth particles, respectively. The diagonal bars correspond to the average of $\hat{x}_i^2$, while the off-diagonal bars represent two-particle position correlations. There are three types of two-particle combinations: both particles from the same subgraph (there are two disconnected subgraphs and thus two different situations) or one particle from each subgraph. Therefore, the three-dimensional bar graph is divided into four regions by two vertical planes. The evolution does not break the exchange symmetry of particles in the subgraphs; thus the correlations between two arbitrary particles from the same subgraph remain the same.

the particles in the evolved eigenstate with $k = (0110100)_2$ after $t = 30$ steps of evolution. The Hamming weights of $(1001010)_2$ and $(0110100)_2$ are identical, and $(0110100)_2$ can be perceived as relabeling particles 1, 4, and 6 as particles 2, 3, and 5 and particles 2, 3, and 5 as particles 1, 4, and 6 in $(1001010)_2$. Referring to the expression of P_{ik} [Eq. (28)], the two eigenstates are essentially the same after the relabeling and therefore have the same position variance, particularly the same second-order term of t.

The bipartite entanglement between part of the coins and all the other degrees of freedom of the seven particles in the initial state $k = (1001010)_2$ is small, compared with that of the evolved state, as shown in Fig. 5. We use the von Neumann entropy as the entanglement measure. The entanglement increases rapidly at the beginning and then starts to oscillate.

VI. CONCLUSIONS

In this paper, we studied the discrete-time multiparticle quantum walk in a one-dimensional lattice, focusing on the position distribution of the particles. We are interested in how fast the relative distance between the particles can increase with time which is a manifestation of the nonclassicality of the quantum walk over its classical counterpart. We used the variance of the position distribution of the particles to quantify the average relative distance between the particles after the evolution of quantum walk, and obtained an asymptotic result of the position variance for a sufficiently large number of time steps.

To explore the limit of spatial propagation of the particles in a quantum walk, we analytically optimized the coin

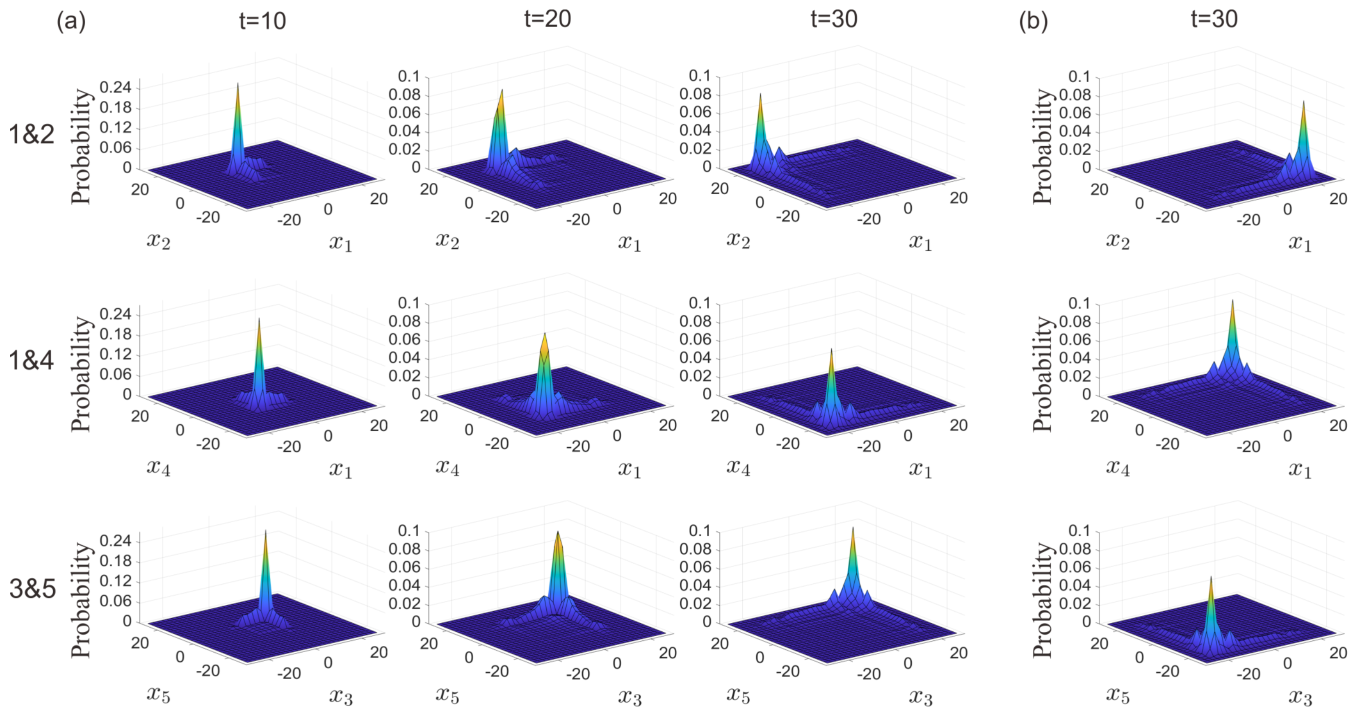

FIG. 4. (a) Two-particle position distributions of particles 1 and 2, 1 and 4, and 3 and 5, in the eigenstate with $k = (1001010)_2$, evolved for $t = 10$, 20, and 30 steps, respectively. For particles 1 and 2, as they belong to different subgraphs, they are more likely to be found in different positions, particularly particle 1 in negative positions and particle 2 in positive positions, since the coins are on average oriented in the opposite directions as can be seen from the initial reduced density matrix of the coins. For two particles in the same subgraph, i.e., 1 and 4, and 3 and 5, on account of the exchange symmetry among particles within the same subgraph, they are close to each other. (b) Two-particle position distributions in the eigenstate associated with $k = (0110100)_2$ after $t = 30$ steps of evolution.

state and derived the upper and lower bounds of the position variance for multiple particles that are initially uncorrelated in the position space but allowed to be entangled in the coin space, and both bounds turn out to scale quadratically with the number of time steps, which is much faster than the linear time scaling in the classical case.

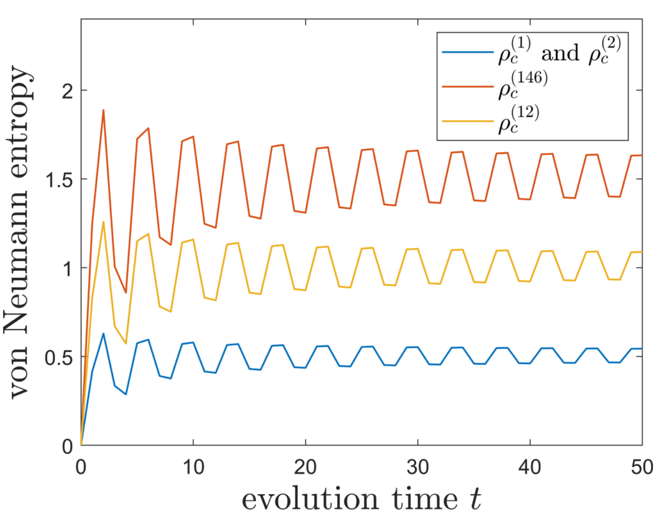

FIG. 5. Bipartite entanglement between the coins denoted in the legend and all the other degrees of freedom of the seven particles over $t = 50$ steps of evolution. For instance, the red line plots the von Neumann entropy for the reduced density matrix $\rho_c^{(146)}$ of the coins of particles 1, 4, and 6. The blue line and the yellow line likewise.

Interesting symmetry in the optimized multiparticle coin states is revealed for the dominant term of position variance: the optimized coin states that extremize the dominant term of position variance possess partial exchange symmetry with respect to two disjoint subsets of the particles; i.e., the optimized coin states are invariant under arbitrary permutation of the particles in either subset. The two subsets of particles in the optimized coin states are correlated, and we studied the entanglement between the two subsets quantified by the von Neumann entropy. We also investigated the position correlations and position distributions of the optimized coin states to reveal more dynamical properties of the quantum walk induced by the partial exchange symmetry.

ACKNOWLEDGMENTS

The authors acknowledge the helpful discussions with Litong Deng from Tsinghua University and Professor Xiaoyong Fu from Sun Yat-sen University. This work is supported by the National Natural Science Foundation of China (Grant No. 12075323), the Innovation Program for Quantum Science and Technology (Grant No. 2021ZD0300702), and the College Students Innovation and Entrepreneurship Training Program, Sun Yat-sen University.

APPENDIX: DETAILS OF THE DERIVATION

In this Appendix, we give more details about the derivation of results in the main text. Section 1 calculates the position variance of multiwalker classical random walks.

Section 2 illustrates the preliminaries of discrete-time multiparticle quantum walks and the process of diagonalizing the evolution operator. Section 3 derives the position variance of the walkers as a function of the evolution time t and initial state. We consider a situation where the particles can be entangled in the coin space, and express the coefficient c_2 of t^2 into matrix multiplication in Sec. 4. Section 5 provides an approach to derive the eigenvalues and eigenvectors of matrix M. We analyze and prove the partial exchange symmetry of the particles of the eigenstates corresponding to the eigenvectors in Sec. 6, and then in Sec. 7 we calculate the bipartite entanglement between the two subsets of particles in which the particles within the same subset possess exchange symmetry.

1. Position variance of multiwalker classical random walk

Considering a classical random walk with n independent walkers, we define the position variance of the particles as

$$\bar{D} = \overline{\sum_{i=1}^{n}\left[x_i - \frac{1}{n}\sum_{j=1}^{n} x_j\right]^2} = \frac{n-1}{n}\sum_i \overline{x_i^2} - \frac{1}{n}\sum_{j\neq k}\bar{x}_j\bar{x}_k. \tag{A1}$$

$x_i = x_{i0} + x_{i1} + \cdots + x_{it}$ is the final position of the ith particle. $x_{it} \in \{-1, 1\}$ is the displacement of the ith particle at step t $(t > 0)$, and the probability of x_{it} to be -1 or 1 is equal. x_{i0} is the initial position of the ith particle. Therefore, $\bar{x}_{it} = 0$ and $\overline{x_{it}^2} = 1$:

$$\begin{aligned}
\bar{D} &= \frac{n-1}{n}\sum_i \overline{(x_{i0} + x_{i1} + x_{i2} + \cdots + x_{it})^2} - \frac{1}{n}\sum_{j\neq k}\bar{x}_j\bar{x}_k \\
&= \frac{n-1}{n}\sum_i \overline{\left(\sum_{\gamma=0}^{t}\sum_{\gamma'=0}^{t} x_{i\gamma}x_{i\gamma'}\right)} - \frac{1}{n}\sum_{j\neq k}\bar{x}_j\bar{x}_k \\
&= \frac{n-1}{n}\sum_i \left[x_{i0}^2 + 2x_{i0}\sum_{\gamma=1}^{t}\bar{x}_{i\gamma} + \sum_{\gamma=1}^{t}\sum_{\gamma'=1,\gamma'\neq\gamma}^{t}\bar{x}_{i\gamma}\bar{x}_{i\gamma'} \right. \\
&\quad \left. + \sum_{\gamma=1}^{t}\overline{x_{i\gamma}^2}\right] - \frac{1}{n}\sum_{j\neq k} x_{j0}x_{k0} \\
&= \frac{n-1}{n}\sum_i x_{i0}^2 - \frac{1}{n}\sum_{j\neq k} x_{j0}x_{k0} + (n-1)t.
\end{aligned} \tag{A2}$$

$\bar{D}$ grows linearly as the function of t.

As for the position variance operator for quantum states, the simplification of Eq. (7) to Eq. (8) is carried out as follows:

$$\begin{aligned}
\hat{D} &= \sum_i\left[\hat{x}_i - \frac{1}{n}\sum_j \hat{x}_j\right]^2 \\
&= \sum_i\left[\hat{x}_i^2 - 2\hat{x}_i\left(\frac{1}{n}\sum_j\hat{x}_j\right) + \left(\frac{1}{n}\sum_j\hat{x}_j\right)^2\right] \\
&= \sum_i \hat{x}_i^2 - 2\sum_i\hat{x}_i\left(\frac{1}{n}\sum_j\hat{x}_j\right) + \sum_i\left(\frac{1}{n}\sum_j\hat{x}_j\right)^2 \\
&= \sum_i \hat{x}_i^2 - 2n\left(\frac{1}{n}\sum_i\hat{x}_i\right)\left(\frac{1}{n}\sum_j\hat{x}_j\right) + n\left(\frac{1}{n}\sum_j\hat{x}_j\right)^2 \\
&= \sum_i \hat{x}_i^2 - \frac{1}{n}\sum_{j,j'}\hat{x}_j\hat{x}_{j'} \\
&= \frac{n-1}{n}\sum_i \hat{x}_i^2 - \frac{1}{n}\sum_{j\neq j'}\hat{x}_j\hat{x}_{j'}.
\end{aligned} \tag{A3}$$

2. Diagonalization of the evolution operator

The n-particle evolution operator is

$$\hat{U}_n = \hat{U}^{\otimes n}, \tag{A4}$$

and $\hat{U} = \hat{S}\cdot(\hat{I}\otimes\hat{C})$, where $\hat{C}$ is the coin operator that flips the coin and $\hat{S}$ is the shift operator that changes the position of the particle according to its coin state. The coin of a particle is also referred to as "spin" wherever no ambiguity occurs. $\hat{S}$ takes the following form: $\hat{S} = \sum_x |x+1\rangle\langle x| \otimes |\uparrow\rangle\langle\uparrow| + \sum_x |x-1\rangle\langle x| \otimes |\downarrow\rangle\langle\downarrow|$.

We perform a discrete-time Fourier transform

$$|K\rangle = \frac{1}{\sqrt{2\pi}}\sum_x e^{iKx}|x\rangle, \tag{A5}$$

where $|K\rangle$ preserves the orthonormality $\langle K'|K\rangle = \delta(K'-K)$, to diagonalize the positional part of the evolution operator in the momentum space that

$$\hat{U}|K\rangle\otimes|s\rangle = |K\rangle\otimes(e^{-iK}|\uparrow\rangle\langle\uparrow| + e^{iK}|\downarrow\rangle\langle\downarrow|)\hat{C}|s\rangle. \tag{A6}$$

The calculation of the evolution can be converted into applying the operator $\hat{U}_K \equiv (e^{-iK}|\uparrow\rangle\langle\uparrow| + e^{iK}|\downarrow\rangle\langle\downarrow|)\hat{C}$ in the coin space. As a specific case, we choose the Hadamard operator $\hat{H}$ as the coin operator:

$$\hat{H} = \frac{1}{\sqrt{2}}(|\uparrow\rangle\langle\uparrow| + |\uparrow\rangle\langle\downarrow| + |\downarrow\rangle\langle\uparrow|) - \frac{1}{\sqrt{2}}|\downarrow\rangle\langle\downarrow|. \tag{A7}$$

Then $\hat{U}_K$ can be written as

$$\hat{U}_K = \frac{e^{-iK}}{\sqrt{2}}(|\uparrow\rangle\langle\uparrow| + |\uparrow\rangle\langle\downarrow|) + \frac{e^{iK}}{\sqrt{2}}(|\downarrow\rangle\langle\uparrow| - |\downarrow\rangle\langle\downarrow|). \tag{A8}$$

By diagonalizing it in the coin space further on, denoting $|d_i(K)\rangle$ as the eigenvectors of the new vector space, the diagonal representation of operator $\hat{U}_K$ is shown in Eq. (A9), where $|d_1\rangle$ and $|d_2\rangle$ are the two eigenvectors:

$$\begin{aligned}
\hat{U}_K &= \frac{e^{-iK}\left(-\sqrt{1+6e^{2iK}+e^{4iK}} - e^{2iK} + 1\right)}{2\sqrt{2}}|d_1\rangle\langle d_1| \\
&\quad + \frac{e^{-iK}\left(\sqrt{1+6e^{2iK}+e^{4iK}} - e^{2iK} + 1\right)}{2\sqrt{2}}|d_2\rangle\langle d_2| \\
&= \lambda_1|d_1\rangle\langle d_1| + \lambda_2|d_2\rangle\langle d_2|.
\end{aligned} \tag{A9}$$

The actual values of λ_1 and λ_2 vary if we choose different branches of the square-root function. Here we define

$$\sqrt{1+6e^{2iK}+e^{4iK}}=\sqrt{2}\cos(K)\sqrt{\cos(2K)+3}+i\sqrt{2}\sin(K)\sqrt{\cos(2K)+3}, \quad (A10)$$

then

$$\lambda_1(K)=-\frac{1}{2}\sqrt{3+\cos(2K)}-\frac{i\sin(K)}{\sqrt{2}},$$
$$\lambda_2(K)=+\frac{1}{2}\sqrt{3+\cos(2K)}-\frac{i\sin(K)}{\sqrt{2}}, \quad (A11)$$
$$|d_1\rangle=-\frac{e^{-iK}}{\sqrt{2N(K)}}|\uparrow\rangle+\frac{1}{\sqrt{2N(\pi-K)}}|\downarrow\rangle, \quad (A12)$$
$$|d_2\rangle=\frac{e^{-iK}}{\sqrt{2N(\pi-K)}}|\uparrow\rangle+\frac{1}{\sqrt{2N(K)}}|\downarrow\rangle, \quad (A13)$$

where $N(K)=(1+\cos^2K)+\cos K\sqrt{1+\cos^2K}=[\sqrt{1+\cos^2K}+\cos K]\sqrt{1+\cos^2K}$. Finally, we arrive at the diagonalized representation of the evolution operator,

$$\hat{U}=\int_{-\pi}^{\pi}\mathrm{d}K|K\rangle\langle K|\otimes(\lambda_1|d_1(K)\rangle\langle d_1(K)|+\lambda_2|d_2(K)\rangle\langle d_2(K)|). \quad (A14)$$

3. Calculation of position variance

As is mentioned in the article, the initial state of an n-particle quantum walk can be written as

$$|\psi_0\rangle=\sum_{x_1s_1\cdots x_ns_n}a_{x_1s_1\cdots x_ns_n}|x_1s_1\rangle|x_2s_2\rangle\cdots|x_ns_n\rangle, \quad (A15)$$

where x_i and s_i are the position and spin of the ith particle.

And the position variance operator is defined as

$$\hat{D}=\sum_i\left[\hat{x}_i-\frac{1}{n}\sum_j\hat{x}_j\right]^2=\frac{n-1}{n}\sum_i\hat{x}_i^2-\frac{1}{n}\sum_{j\neq j'}\hat{x}_j\hat{x}_{j'}, \quad (A16)$$

consisting of single-particle operators and two-particle operators. Similar to evolving operators in the Heisenberg picture, the evolved position variance operator can be decomposed into the summation of single-particle operators and two-particle operators:

$$(\hat{U}_n^\dagger)^t\hat{D}\hat{U}_n^t=\frac{n-1}{n}\sum_i(\hat{U}_i^\dagger)^t\hat{x}_i^2\hat{U}_i^t-\frac{1}{n}\sum_{j\neq k}(\hat{U}_j^\dagger)^t\hat{x}_j\hat{U}_j^t\otimes(\hat{U}_k^\dagger)^t\hat{x}_k\hat{U}_k^t. \quad (A17)$$

The subscripts i, j, k represent which particle the operators apply on. The position variance after t steps of evolution is given by

$$\langle\psi_0|(\hat{U}_n^\dagger)^t\hat{D}\hat{U}_n^t|\psi_0\rangle=\sum_{x_1's_1'\cdots x_n's_n'}\sum_{x_1s_1\cdots x_ns_n}a^*_{x_1's_1'\cdots x_n's_n'}a_{x_1s_1\cdots x_ns_n}\left[\frac{n-1}{n}\sum_i\langle x_i's_i'|(\hat{U}^\dagger)^t\hat{x}_i^2\hat{U}^t|x_is_i\rangle\prod_{\gamma=1,\gamma\neq i}^{n}\delta_{x_\gamma's_\gamma',x_\gamma s_\gamma}\right.$$
$$\left.-\frac{1}{n}\sum_{j\neq k}\langle x_j's_j'|(\hat{U}^\dagger)^t\hat{x}_j\hat{U}^t|x_js_j\rangle\langle x_k's_k'|(\hat{U}^\dagger)^t\hat{x}_k\hat{U}^t|x_ks_k\rangle\prod_{\gamma=1,\gamma\neq j,k}^{n}\delta_{x_\gamma's_\gamma',x_\gamma s_\gamma}\right]. \quad (A18)$$

$\delta_{x_\gamma's_\gamma',x_\gamma s_\gamma}$ is 1 if $x_\gamma'=x_\gamma$ and $s_\gamma'=s_\gamma$, and is 0 otherwise, implying the summands $\langle x_i's_i'|(\hat{U}^\dagger)^t\hat{x}_i^2\hat{U}^t|x_is_i\rangle$ can contribute to the position variance only when the states of the particles other than the ith particle in the bra $\langle x_1's_1'|\cdots\langle x_n's_n'|$ and the ket $|x_1s_1\rangle\cdots|x_ns_n\rangle$ match. A similar constraint applies to the summands $\langle x_j's_j'|(\hat{U}^\dagger)^t\hat{x}_j\hat{U}^t|x_js_j\rangle\langle x_k's_k'|(\hat{U}^\dagger)^t\hat{x}_k\hat{U}^t|x_ks_k\rangle$. For the single-particle term, the matrix elements can be further derived through the following procedure,

$$\langle x_i's_i'|(\hat{U}^\dagger)^t\hat{x}_i^2\hat{U}^t|x_is_i\rangle=\int_{-\pi}^{\pi}\int_{-\pi}^{\pi}\mathrm{d}K'\mathrm{d}K\sum_{d,d'}\langle x_i's_i'|K'd'\rangle\langle K'd'|(\hat{U}^\dagger)^t\hat{x}_i^2\hat{U}^t|Kd\rangle\langle Kd|x_is_i\rangle$$
$$=\int_{-\pi}^{\pi}\int_{-\pi}^{\pi}\mathrm{d}K'\mathrm{d}K\sum_{d,d'}\langle x_i'|K'\rangle\langle s_i'|d'\rangle\langle K|x_i\rangle\langle d|s_i\rangle\langle d'|(\hat{U}_{K'}^\dagger)^t|d'\rangle\langle K'|\hat{x}_i^2|K\rangle\langle d'|d\rangle\langle d|\hat{U}_K^t|d\rangle$$
$$=-\frac{1}{2\pi}\int_{-\pi}^{\pi}\int_{-\pi}^{\pi}\mathrm{d}K'\mathrm{d}K\sum_{d,d'}e^{iK'x_i'}e^{-iKx_i}\langle s_i'|d'\rangle\langle d|s_i\rangle\langle d'|(\hat{U}_{K'}^\dagger)^t|d'\rangle\delta^{(2)}(K'-K)\langle d'|d\rangle\langle d|\hat{U}_K^t|d\rangle$$
$$=-\frac{1}{2\pi}\int_{-\pi}^{\pi}\mathrm{d}K\sum_{d,d'}\partial_{K'}^2[e^{i(K'x_i'-Kx_i)}\langle s_i'|d'\rangle\langle d|s_i\rangle\lambda_{d'}^*(K')^t\lambda_d(K)^t\langle d'(K')|d(K)\rangle]|_{K'=K}. \quad (A19)$$

We used

$$\langle K'|\hat{x}_i^2|K\rangle=\sum_{x=-\infty}^{\infty}\langle K'|\hat{x}_i^2|x\rangle\langle x|K\rangle=\frac{1}{2\pi}\sum_{x=-\infty}^{\infty}x^2e^{-i(K'-K)x}=-\sum_{l=-\infty}^{\infty}\delta^{(2)}(K'-K+2\pi l), \quad (A20)$$

$l \in \mathbb{Z}$, where we utilized the relation

$$\frac{1}{2\pi}\sum_{x=-\infty}^{\infty} x^m e^{-i(K'-K)x} = (i)^m \sum_{l=-\infty}^{\infty} \delta^{(m)}(K'-K+2\pi l), \tag{A21}$$

which is the periodic extension of the derivative of the Dirac delta function with period 2π. We can omit the summation on the right-hand side because the integration region is 2π, so there is one term remaining. Then we can use $\langle K'|\hat{x}_i^2|K\rangle = -\delta^{(2)}(K'-K)$ in the integral.

The order of t is relative to the order of derivatives. If we expand the derivatives,

$$\begin{aligned}
&\langle x_i's_i'|(\hat{U}^\dagger)^t\hat{x}_i^2\hat{U}^t|x_is_i\rangle \\
&= -\frac{1}{2\pi}\int_{-\pi}^{\pi}\mathrm{d}K\sum_{d,d'}\partial_{K'}^2[e^{iK'x_i'}\langle s_i'|d'\rangle\lambda_{d'}^*(K')^t\langle d'(K')|d(K)\rangle]|_{K'=K}e^{-iKx_i}\langle d|s_i\rangle\lambda_d(K)^t \\
&= -\frac{1}{2\pi}\int_{-\pi}^{\pi}\mathrm{d}K\sum_{d,d'}\big\{\partial_{K'}^2[e^{iK'x_i'}\langle s_i'|d'\rangle\langle d'(K')|d(K)\rangle]\lambda_{d'}^*(K')^t + 2\partial_{K'}[e^{iK'x_i'}\langle s_i'|d'\rangle\langle d'(K')|d(K)\rangle]\partial_{K'}[\lambda_{d'}^*(K')^t] \\
&\quad + e^{iK'x_i'}\langle s_i'|d'\rangle\langle d'(K')|d(K)\rangle\partial_{K'}^2[\lambda_{d'}^*(K')^t]\big\}|_{K'=K}e^{-iKx_i}\langle d|s_i\rangle\lambda_d(K)^t \\
&= -\frac{1}{2\pi}\int_{-\pi}^{\pi}\mathrm{d}K\sum_{d}\big\{\partial_{K'}^2[e^{iK'x_i'}\langle s_i'|d(K')\rangle\langle d(K')|d(K)\rangle]\lambda_{d}^*(K')^t + 2\partial_{K'}[e^{iK'x_i'}\langle s_i'|d(K')\rangle\langle d(K')|d(K)\rangle]\partial_{K'}[\lambda_{d}^*(K')^t] \\
&\quad + e^{iK'x_i'}\langle s_i'|d(K')\rangle\langle d(K')|d(K)\rangle\partial_{K'}^2[\lambda_{d}^*(K')^t]\big\}|_{K'=K}e^{-iKx_i}\langle d(K)|s_i\rangle\lambda_d(K)^t \\
&\quad - \frac{1}{2\pi}\int_{-\pi}^{\pi}\mathrm{d}K\sum_{d\neq d'}\big\{\partial_{K'}^2[e^{iK'x_i'}\langle s_i'|d'(K')\rangle\langle d'(K')|d(K)\rangle]\lambda_{d'}^*(K')^t + 2\partial_{K'}[e^{iK'x_i'}\langle s_i'|d'(K')\rangle\langle d'(K')|d(K)\rangle]\partial_{K'}[\lambda_{d'}^*(K')^t] \\
&\quad + e^{iK'x_i'}\langle s_i'|d'(K')\rangle\langle d'(K')|d(K)\rangle\partial_{K'}^2[\lambda_{d'}^*(K')^t]\big\}|_{K'=K}e^{-iKx_i}\langle d(K)|s_i\rangle\lambda_d(K)^t \\
&= -\frac{1}{2\pi}\int_{-\pi}^{\pi}\mathrm{d}K\sum_{d}\big\{\partial_{K'}^2[e^{iK'x_i'}\langle s_i'|d(K')\rangle\langle d(K')|d(K)\rangle]|_{K'=K}e^{-iKx_i}\langle d(K)|s_i\rangle \\
&\quad + 2\partial_{K'}[e^{iK'x_i'}\langle s_i'|d(K')\rangle\langle d(K')|d(K)\rangle]|_{K'=K}t\lambda_d^*(K)^{-1}\partial_K[\lambda_d^*(K)]e^{-iKx_i}\langle d(K)|s_i\rangle \\
&\quad + e^{iK(x_i'-x_i)}\langle s_i'|d(K)\rangle t(t-1)\lambda_d^*(K)^{-2}\langle d(K)|s_i\rangle(\partial_K[\lambda_d^*(K)])^2 + e^{iK(x_i'-x_i)}\langle s_i'|d(K)\rangle\langle d(K)|s_i\rangle t\lambda_d^*(K)^{-1}\partial_K^2[\lambda_d^*(K)]\big\}\big\} \\
&\quad - \frac{1}{2\pi}\int_{-\pi}^{\pi}\mathrm{d}K\sum_{d\neq d'}\big\{\partial_{K'}^2[e^{iK'x_i'}\langle s_i'|d'(K')\rangle\langle d'(K')|d(K)\rangle]|_{K'=K} \\
&\quad + 2\partial_{K'}[e^{iK'x_i'}\langle s_i'|d'(K')\rangle\langle d'(K')|d(K)\rangle]|_{K'=K}t\lambda_{d'}^*(K)^{-1}\partial_K[\lambda_{d'}^*(K)] \\
&\quad + e^{iKx_i'}\langle s_i'|d'(K)\rangle\langle d'(K)|d(K)\rangle\{t(t-1)\lambda_{d'}^*(K)^{-2}(\partial_K[\lambda_{d'}^*(K)])^2 + t\lambda_{d'}^*(K)^{-1}\partial_K^2[\lambda_{d'}^*(K)]\}\big\}e^{-iKx_i}\langle d(K)|s_i\rangle\lambda_{d'}^*(K)^t\lambda_d(K)^t \\
&= -\frac{1}{2\pi}[t^2I_{A2}(x_i'-x_i,s_i',s_i) + tI_{A1}(x_i',x_i,s_i',s_i) + I_{AC}(x_i',x_i,s_i',s_i) + I_{Ao}(x_i',x_i,s_i',s_i;t)].
\end{aligned} \tag{A22}$$

Denote

$$I_{A2}(x_i'-x_i,s_i',s_i) = \int_{-\pi}^{\pi}\mathrm{d}K e^{iK(x_i'-x_i)}\sum_d\langle s_i'|d(K)\rangle\langle d(K)|s_i\rangle\lambda_d^*(K)^{-2}(\partial_K[\lambda_d^*(K)])^2, \tag{A23}$$

$$\begin{aligned}
I_{A1}(x_i',x_i,s_i',s_i) = \int_{-\pi}^{\pi}\mathrm{d}K\sum_d\{&2\partial_{K'}[e^{iK'x_i'}\langle s_i'|d(K')\rangle\langle d(K')|d(K)\rangle]|_{K'=K}\lambda_d^*(K)^{-1}\partial_K[\lambda_d^*(K)]e^{-iKx_i}\langle d(K)|s_i\rangle \\
&+ e^{iK(x_i'-x_i)}\langle s_i'|d(K)\rangle\langle d(K)|s_i\rangle\{-\lambda_d^*(K)^{-2}(\partial_K[\lambda_d^*(K)])^2 + \lambda_d^*(K)^{-1}\partial_K^2[\lambda_d^*(K)]\}\},
\end{aligned} \tag{A24}$$

$$I_{AC}(x_i',x_i,s_i',s_i) = \int_{-\pi}^{\pi}\mathrm{d}K\sum_d\partial_{K'}^2[e^{iK'x_i'}\langle s_i'|d(K')\rangle\langle d(K')|d(K)\rangle]|_{K'=K}e^{-iKx_i}\langle d(K)|s_i\rangle, \tag{A25}$$

$$\begin{aligned}
I_{Ao}(x_i',x_i,s_i',s_i;t) = \int_{-\pi}^{\pi}\mathrm{d}K\sum_{d\neq d'}\{&\partial_{K'}^2[e^{iK'x_i'}\langle s_i'|d'(K')\rangle\langle d'(K')|d(K)\rangle]|_{K'=K} \\
&+ 2\partial_{K'}[e^{iK'x_i'}\langle s_i'|d'(K')\rangle\langle d'(K')|d(K)\rangle]|_{K'=K}t\lambda_{d'}^*(K)^{-1}\partial_K[\lambda_{d'}^*(K)]\}e^{-iKx_i}\langle d(K)|s_i\rangle(\lambda_{d'}^*(K)\lambda_d(K))^t.
\end{aligned} \tag{A26}$$

And for the other term,

$$\begin{aligned}
&\langle x_i' s_i'|(\hat{U}^\dagger)^t \hat{x}_i \hat{U}^t|x_i s_i\rangle \\
&= \int_{-\pi}^{\pi}\int_{-\pi}^{\pi} \mathrm{d}K'\mathrm{d}K \sum_{d,d'} \langle x_i' s_i'|K'd'\rangle\langle K'd'|(\hat{U}^\dagger)^t \hat{x}_i \hat{U}^t|Kd\rangle\langle Kd|x_i s_i\rangle \\
&= \int_{-\pi}^{\pi}\int_{-\pi}^{\pi} \mathrm{d}K'\mathrm{d}K \sum_{d,d'} \langle x_i'|K'\rangle\langle s_i'|d'\rangle\langle K|x_i\rangle\langle d|s_i\rangle\langle d'|(\hat{U}_{K'}^\dagger)^t|d'\rangle\langle K'|\hat{x}_i|K\rangle\langle d'|d\rangle\langle d|\hat{U}_K^t|d\rangle \\
&= \frac{i}{2\pi}\int_{-\pi}^{\pi}\int_{-\pi}^{\pi} \mathrm{d}K'\mathrm{d}K \sum_{d,d'} e^{iK'x_i'}e^{-iKx_i}\langle s_i'|d'\rangle\langle d|s_i\rangle\langle d'|(\hat{U}_{K'}^\dagger)^t|d'\rangle\delta^{(1)}(K'-K)\langle d'|d\rangle\langle d|\hat{U}_K^t|d\rangle \\
&= -\frac{i}{2\pi}\int_{-\pi}^{\pi} \mathrm{d}K \sum_{d,d'} \partial_{K'}[e^{i(K'x_i'-Kx_i)}\langle s_i'|d'\rangle\langle d|s_i\rangle\lambda_{d'}^*(K')^t\lambda_d(K)^t\langle d'(K')|d(K)\rangle]|_{K'=K}.
\end{aligned} \tag{A27}$$

Similarly,

$$\begin{aligned}
\langle x_i' s_i'|(\hat{U}^\dagger)^t \hat{x}_i \hat{U}^t|x_i s_i\rangle &= -\frac{i}{2\pi}\int_{-\pi}^{\pi} \mathrm{d}K \sum_{d,d'} \{\partial_{K'}[e^{iK'x_i'}\langle s_i'|d'(K')\rangle\langle d'(K')|d(K)\rangle]\lambda_{d'}^*(K')^t \\
&\quad + e^{iK'x_i'}\langle s_i'|d'(K')\rangle\langle d'(K')|d(K)\rangle\partial_{K'}[\lambda_{d'}^*(K')^t]\}|_{K'=K}e^{-iKx_i}\langle d(K)|s_i\rangle\lambda_d(K)^t \\
&= -\frac{i}{2\pi}\int_{-\pi}^{\pi} \mathrm{d}K \sum_{d} \{\partial_{K'}[e^{iK'x_i'}\langle s_i'|d(K')\rangle\langle d(K')|d(K)\rangle]\lambda_{d}^*(K')^t \\
&\quad + e^{iK'x_i'}\langle s_i'|d(K')\rangle\langle d(K')|d(K)\rangle\partial_{K'}[\lambda_{d}^*(K')^t]\}|_{K'=K}e^{-iKx_i}\langle d(K)|s_i\rangle\lambda_d(K)^t \\
&\quad - \frac{i}{2\pi}\int_{-\pi}^{\pi} \mathrm{d}K \sum_{d'\neq d} \{\partial_{K'}[e^{iK'x_i'}\langle s_i'|d'(K')\rangle\langle d'(K')|d(K)\rangle]|_{K'=K}\lambda_{d'}^*(K)^t \\
&\quad + e^{iKx_i'}\langle s_i'|d'(K)\rangle\langle d'(K)|d(K)\rangle\partial_{K'}[\lambda_{d'}^*(K')^t]|_{K'=K}\}e^{-iKx_i}\langle d(K)|s_i\rangle\lambda_d(K)^t \\
&= -\frac{i}{2\pi}\int_{-\pi}^{\pi} \mathrm{d}K \sum_{d} \{\partial_{K'}[e^{iK'x_i'}\langle s_i'|d(K')\rangle\langle d(K')|d(K)\rangle]|_{K'=K}\lambda_{d}^*(K)^t \\
&\quad + e^{iKx_i'}\langle s_i'|d(K)\rangle\partial_{K'}[\lambda_{d}^*(K')^t]|_{K'=K}\}e^{-iKx_i}\langle d(K)|s_i\rangle\lambda_d(K)^t \\
&\quad - \frac{i}{2\pi}\int_{-\pi}^{\pi} \mathrm{d}K \sum_{d'\neq d} \partial_{K'}[e^{iK'x_i'}\langle s_i'|d'(K')\rangle\langle d'(K')|d(K)\rangle]|_{K'=K}e^{-iKx_i}\langle d(K)|s_i\rangle(\lambda_{d'}^*(K)\lambda_d(K))^t \\
&= -\frac{i}{2\pi}[tI_B(x_i'-x_i,s_i',s_i) + I_{B_1}(x_i',x_i,s_i',s_i) + I_{Bo}(x_i',x_i,s_i',s_i;t)],
\end{aligned} \tag{A28}$$

$$I_B(x_i'-x_i,s_i',s_i) = \int_{-\pi}^{\pi} \mathrm{d}K \sum_{d} e^{iK(x_i'-x_i)}\langle s_i'|d(K)\rangle\langle d(K)|s_i\rangle\lambda_d^*(K)^{-1}\partial_K[\lambda_d^*(K)], \tag{A29}$$

$$\begin{aligned}
I_{B_1}(x_i',x_i,s_i',s_i) &= \int_{-\pi}^{\pi} \mathrm{d}K \sum_{d} \partial_{K'}[e^{iK'x_i'}\langle s_i'|d(K')\rangle\langle d(K')|d(K)\rangle]|_{K'=K}e^{-iKx_i}\langle d(K)|s_i\rangle \\
&= \int_{-\pi}^{\pi} \mathrm{d}K \sum_{d} \{\partial_{K'}[e^{iK'x_i'}\langle s_i'|d(K')\rangle]|_{K'=K} + e^{iKx_i'}\langle s_i'|d(K)\rangle\partial_{K'}[\langle d(K')|d(K)\rangle]|_{K'=K}\}e^{-iKx_i}\langle d(K)|s_i\rangle,
\end{aligned} \tag{A30}$$

$$\begin{aligned}
I_{Bo}(x_i',x_i,s_i',s_i;t) &= \int_{-\pi}^{\pi} \mathrm{d}K \sum_{d\neq d'} \partial_{K'}[e^{iK'x_i'}\langle s_i'|d'(K')\rangle\langle d'(K')|d(K)\rangle]|_{K'=K}e^{-iKx_i}\langle d(K)|s_i\rangle(\lambda_{d'}^*(K)\lambda_d(K))^t \\
&= \int_{-\pi}^{\pi} \mathrm{d}K \sum_{d\neq d'} e^{iK(x_i'-x_i)}\langle s_i'|d'(K)\rangle\langle d(K)|s_i\rangle\partial_{K'}[\langle d'(K')|d(K)\rangle]|_{K'=K}(\lambda_{d'}^*(K)\lambda_d(K))^t.
\end{aligned} \tag{A31}$$

The above expressions can apply to any coin operator of SU(2) with $\lambda_d(K)$ and $|d(K)\rangle$ computed from the conditional unitary operator $\hat{U}_K$ with the new coin operator. If we use the Hadamard coin,

$$I_{A2}(x'-x,s',s)=\begin{cases}(\sqrt{2}-2)\pi, & x'-x=0,\ s'=s\\ \sqrt{2}\pi(\sqrt{2}-1)^{|x'-x|}\cos\left(\frac{\pi(x'-x)}{2}\right), & x'-x\neq 0,\ s'=s\\ 0, & s'\neq s\end{cases}$$
$$=\begin{cases}(1-\sqrt{2})f(0), & x'-x=0,\ s'=s\\ f(x'-x), & x'-x\neq 0,\ s'=s\\ 0, & s'\neq s,\end{cases} \tag{A32}$$

where $f(x)=\sqrt{2}\pi(\sqrt{2}-1)^{|x|}\cos(\pi x/2)$.

$$I_{A1}(x',x,s',s)=\begin{cases}16x'[I_a(\Delta x-2)+I_a(\Delta x+2)]+28x'I_a(\Delta x) & \\ \quad +2x'[I_a(\Delta x+4)+I_a(\Delta x-4)]+8[I_a(\Delta x+2)-I_a(\Delta x-2)], & s'=s=\uparrow\\ -\{16x'[I_a(\Delta x-2)+I_a(\Delta x+2)]+28x'I_a(\Delta x) & \\ \quad +2x'[I_a(\Delta x+4)+I_a(\Delta x-4)]+8[I_a(\Delta x+2)-I_a(\Delta x-2)]\}, & s'=s=\downarrow\\ (4x'-4)I_a(\Delta x+2)+(28x'-8)I_a(\Delta x)+(28x'-20)I_a(\Delta x-2)+4x'I_a(\Delta x-4), & s'=\uparrow,\ s=\downarrow\\ (4x'+4)I_a(\Delta x-2)+(28x'+8)I_a(\Delta x)+(28x'+20)I_a(\Delta x+2)+4x'I_a(\Delta x+4), & s'=\downarrow,\ s=\uparrow,\end{cases} \tag{A33}$$

$$I_{AC}(x',x,s',s)=\begin{cases}x'^2I_a(x'-x-4)-4(1+x'-3x'^2)I_a(x'-x-2)+(16-24x'+38x'^2)I_a(x'-x) & \\ \quad +4(1-x'+3x'^2)I_a(x'-x+2)+x'^2I_a(x'-x+4), & s'=s=\uparrow\\ x'^2I_a(x'-x-4)+4(1+x'+3x'^2)I_a(x'-x-2)+(16+24x'+38x'^2)I_a(x'-x) & \\ \quad +4(-1+x'+3x'^2)I_a(x'-x+2)+x'^2I_a(x'-x+4), & s'=s=\downarrow\\ 4(1+x')I_a(x'-x-2)+24x'I_a(x'-x)+4(x'-1)I_a(x'-x+2), & s'\neq s,\end{cases} \tag{A34}$$

where $\Delta x=x'-x$, $I_a(x)=-\frac{\pi}{64}(\sqrt{2}-1)^{|x|}(3\sqrt{2}+2|x|)\cos(\frac{\pi x}{2})$.

$$I_{Ao}(x',x,s',s;t)$$
$$=\begin{cases}(-1)^{\frac{3}{4}}\sqrt{\frac{\pi}{4t}}e^{-\frac{1}{2}i\pi(3t+x'+x)}((-1+(1+i)x')(e^{i\pi(t+x)}+e^{i\pi(3t+x')})+((1+i)x'-i)(e^{i\pi(2t+x)}+e^{i\pi x'})), & s'=s=\uparrow\\ -(-1)^{\frac{3}{4}}\sqrt{\frac{\pi}{4t}}e^{-\frac{1}{2}i\pi(3t+x'+x)}((1+(1+i)x')(e^{i\pi(t+x)}+e^{i\pi(3t+x')})+((1+i)x'+i)(e^{i\pi(2t+x)}+e^{i\pi x'})), & s'=s=\downarrow\\ (-1)^{\frac{1}{4}}\sqrt{\frac{\pi}{4t}}e^{-\frac{1}{2}i\pi(3t+x'+x)}(((1+i)x'-i)(e^{i\pi(2t+x)}+e^{i\pi x'})+(1-(1+i)x')(e^{i\pi(t+x)}+e^{i\pi(3t+x')})), & s'=\uparrow,\ s=\downarrow\\ (-1)^{\frac{3}{4}}\sqrt{\frac{\pi}{4t}}e^{-\frac{1}{2}i\pi(3t+x'+x)}((1+(1-i)x')(e^{i\pi(2t+x)}+e^{i\pi x'})+i(1+(1+i)x')(e^{i\pi(t+x)}+e^{i\pi(3t+x')})), & s'=\downarrow,\ s=\uparrow\end{cases}$$
$$+\,o\left(\sqrt{\frac{1}{t}}\right). \tag{A35}$$

$$I_B(x'-x,s',s)=\begin{cases}-iI_{A2}(x'-x,s',s), & s'=s=\uparrow\\ iI_{A2}(x'-x,s',s), & s'=s=\downarrow\\ \frac{i\pi}{\sqrt{2}}\cos\left(\frac{\pi(x'-x)}{2}\right)[(\sqrt{2}-1)^{|x'-x|}-(\sqrt{2}-1)^{|x'-x-2|}], & s'=\uparrow,\ s=\downarrow\\ \frac{i\pi}{\sqrt{2}}\cos\left(\frac{\pi(x'-x)}{2}\right)[(\sqrt{2}-1)^{|x'-x|}-(\sqrt{2}-1)^{|x'-x+2|}], & s'=\downarrow,\ s=\uparrow\end{cases}$$
$$=\begin{cases}(-1)^s iI_{A2}(x'-x,s',s), & s'=s\\ \frac{i}{2}[f(x'-x)+f(x'-x-(-1)^s\times 2)], & s'\neq s.\end{cases} \tag{A36}$$

In the above equation, when s is $\uparrow$, it acts as number 1, and $\downarrow$ as number 0; i.e., when $s=\uparrow$, $(-1)^s=-1$, and when $s=\downarrow$, $(-1)^s=1$.

$$I_{B_1}(x',x,s',s)=\begin{cases}2i\pi x\delta_{x'-x,0}-\frac{i\pi\left(\sqrt{2}-1\right)^{|x'-x|}\cos\left(\frac{\pi(x'-x)}{2}\right)}{\sqrt{2}}, & s'=s=\uparrow\\ 2i\pi x\delta_{x'-x,0}+\frac{i\pi\left(\sqrt{2}-1\right)^{|x'-x|}\cos\left(\frac{\pi(x'-x)}{2}\right)}{\sqrt{2}}, & s'=s=\downarrow\\ \frac{i\pi\left(\sqrt{2}-1\right)^{|x'-x|}\cos\left(\frac{\pi(x'-x)}{2}\right)}{\sqrt{2}}, & s'\neq s.\end{cases} \tag{A37}$$

$$I_{Bo}(x',x,s',s;t)=\begin{cases}\frac{1}{2}i\sqrt{\frac{\pi}{2t}}(1+e^{i\pi t})e^{-\frac{1}{2}i\pi(3t+x'+x)}(-e^{i\pi(t+x')}+e^{i\pi(2t+x')}+e^{i\pi(t+x)}+e^{i\pi x'}), & s'=s=\uparrow\\ -\frac{1}{2}i\sqrt{\frac{\pi}{2t}}(1+e^{i\pi t})e^{-\frac{1}{2}i\pi(3t+x'+x)}(-e^{i\pi(t+x')}+e^{i\pi(2t+x')}+e^{i\pi(t+x)}+e^{i\pi x'}), & s'=s=\downarrow\\ -\frac{1}{2}\sqrt{\frac{\pi}{2t}}(-1+e^{i\pi t})e^{-\frac{1}{2}i\pi(3t+x'+x)}(e^{i\pi(t+x')}+e^{i\pi(2t+x')}-e^{i\pi(t+x)}+e^{i\pi x'}), & s'=\uparrow, s=\downarrow\\ -\frac{1}{2}\sqrt{\frac{\pi}{2t}}(-1+e^{i\pi t})e^{-\frac{1}{2}i\pi(3t+x'+x)}(e^{i\pi(t+x')}+e^{i\pi(2t+x')}-e^{i\pi(t+x)}+e^{i\pi x'}), & s'=\downarrow, s=\uparrow\end{cases}+o\left(\sqrt{\frac{1}{t}}\right). \tag{A38}$$

I_{Ao} and I_{Bo} are integrals with rapidly varying phase when t is large, and they approach zero when $t\to\infty$. But note that in the expression of $\langle\hat{D}\rangle$, there are terms of I_{Bo} multiplied by t, and this results in the terms of order $\sqrt{t}$. The asymptotic formula can be calculated by stationary phase approximation. Let Ω denote the set of critical points of a real function $f(x)$ in the region (a,b) and $t>0$, and assume $g(x)$ is compactly supported or has exponential decay. Then,

$$\int_a^b g(x)e^{itf(x)}\mathrm{d}x=\sum_{x_0\in\Omega}g(x_0)e^{itf(x_0)+\mathrm{sign}(f''(x_0))\frac{i\pi}{4}}\left(\frac{2\pi}{t|f''(x_0)|}\right)^{\frac{1}{2}}+o(t^{-\frac{1}{2}}). \tag{A39}$$

To illustrate how we calculate the integrals like I_{A2}, I_{A1}, I_{AC}, I_B, and I_{B_1} using the residue theorem, we give an example of calculating the integral

$$I_{A2}(x'-x,s',s)=\int_{-\pi}^{\pi}\mathrm{d}Ke^{iK(x'-x)}\sum_d\langle s'|d(K)\rangle\langle d(K)|s\rangle\lambda_d^*(K)^{-2}(\partial_K[\lambda_d^*(K)])^2. \tag{A40}$$

When $s'=s$,

$$I_{A2}(x'-x,s',s)=\int_{-\pi}^{\pi}\left[-\frac{2e^{iK(x'-x)}\cos^2(K)}{\cos(2K)+3}\right]\mathrm{d}K\overset{z=e^{iK}}{=}\oint_{|z|=1}\left[i\frac{z^{(x'-x-1)}(z+z^{-1})^2}{((z+z^{-1})^2+4)}\right]\mathrm{d}z=\oint_{|z|=1}i\left[z^{(x'-x-1)}-\frac{4z^{(x'-x+1)}}{z^4+6z^2+1}\right]\mathrm{d}z. \tag{A41}$$

The roots of the equation $z^4+6z^2+1=0$ are $-i(\sqrt{2}-1)$, $i(\sqrt{2}-1)$, $-i(\sqrt{2}+1)$, $i(\sqrt{2}+1)$, among which $-i(\sqrt{2}-1)$, $i(\sqrt{2}-1)$ are inside the unit circle on the complex plane and $-i(\sqrt{2}+1)$, $i(\sqrt{2}+1)$ are outside. They are the first-order poles of the integrand. In addition, $z^{(x'-x-1)}$ may produce a residue when $x'-x-1=-1$. Then

$$\begin{aligned}I_{A2}(x'-x,s',s)&=\begin{cases}-2\pi i\{\mathrm{Res}[f(-i\sqrt{3+2\sqrt{2}})]+\mathrm{Res}[f(i\sqrt{3+2\sqrt{2}})]\}, & x'-x<0\\ +2\pi i\{\mathrm{Res}[f(-i\sqrt{3-2\sqrt{2}})]+\mathrm{Res}[f(i\sqrt{3-2\sqrt{2}})]\}-2\pi i\mathrm{Res}[f(\infty)], & x'-x=0\\ +2\pi i\{\mathrm{Res}[f(-i\sqrt{3-2\sqrt{2}})]+\mathrm{Res}[f(i\sqrt{3-2\sqrt{2}})]\}, & x'-x>0,\end{cases}\\ &=\begin{cases}\sqrt{2}\pi(3+2\sqrt{2})^{(x'-x)/2}\cos\left(\frac{\pi(x'-x)}{2}\right), & x'-x<0\\ (\sqrt{2}-2)\pi, & x'-x=0\\ \sqrt{2}\pi(3-2\sqrt{2})^{(x'-x)/2}\cos\left(\frac{\pi(x'-x)}{2}\right), & x'-x>0\end{cases}\\ &=\begin{cases}(\sqrt{2}-2)\pi, & x'-x=0\\ \sqrt{2}\pi(3-2\sqrt{2})^{|x'-x|/2}\cos\left(\frac{\pi(x'-x)}{2}\right), & x'-x\neq 0.\end{cases}\end{aligned} \tag{A42}$$

The notation $\mathrm{Res}[f(a)]$ represents the residue of function $f(z)$ at point a. When $s'\neq s$,

$$I_{A2}(x'-x,s',s)=0. \tag{A43}$$

To sum up,

$$I_{A2}(x'-x,s',s)=\begin{cases}(\sqrt{2}-2)\pi, & x'-x=0, s'=s\\ \sqrt{2}\pi(\sqrt{2}-1)^{|x'-x|}\cos\left(\frac{\pi(x'-x)}{2}\right), & x'-x\neq 0, s'=s\\ 0, & s'\neq s.\end{cases} \tag{A44}$$

4. Optimization problem of coefficient

The coefficient c_2 of t^2 in the expression of the position variance after t steps of evolution $\langle\Psi|(\hat{U}^\dagger)^t\hat{D}\hat{U}^t|\Psi\rangle$ can be calculated from the combination of inner products of $\langle x_1s_1'|\cdots\langle x_ns_n'|(\hat{U}_n^\dagger)^t\hat{D}\hat{U}_n^t|x_1s_1\rangle\cdots|x_ns_n\rangle$ [see Eq. (A45)]. For simplicity, we regard $\uparrow$ as number 1 and $\downarrow$ as number 0 and denote the spin of the ith particle as $|s_i\rangle$. Then the vector $|s_i\rangle$ takes on the value of $|1\rangle$ or $|0\rangle$, and the combination of the spin notations of these particles can be treated as a binary number whose numerical value is ξ, that is, $|s_1s_2\cdots s_n\rangle=|2^{n-1}\times s_1+2^{n-2}\times s_2+\cdots+2s_{n-1}+s_n\rangle=|\xi\rangle$. We can rewrite the basis state vectors as $|x_1\rangle|x_2\rangle\cdots|x_n\rangle|\xi\rangle$.

The position variance is given by

$$\langle\Psi|(\hat{U}^{\dagger})\hat{D}\hat{U}^{t}|\Psi\rangle = \left[\langle x_1|\langle x_2|\cdots\langle x_n|\sum_{\xi'=0}^{2^n-1} a^*_{\xi'}\langle\xi'|\right](\hat{U}^{\dagger}_n)^t\hat{D}\hat{U}^t_n\left[|x_1\rangle|x_2\rangle\cdots|x_n\rangle\sum_{\xi=0}^{2^n-1} a_{\xi}|\xi\rangle\right], \quad \text{(A45)}$$

in which the coefficient of t^2 is

$$c_2 = \sum_{\xi'\xi} a^*_{\xi'}a_{\xi}M_{\xi'\xi} = [a^*_0, a^*_1, \dots, a^*_{2^n-1}]M\begin{bmatrix} a_0 \\ a_1 \\ \vdots \\ a_{2^n-1}\end{bmatrix}. \quad \text{(A46)}$$

The matrix elements of M are given by

$$M_{\xi'\xi} = -\frac{n-1}{n}\frac{1}{2\pi}\sum_i I_{A2}(0, s'_i, s_i)\prod_{\gamma=1,\gamma\neq i}^{n}\delta_{x'_{\gamma}s'_{\gamma},x_{\gamma}s_{\gamma}} + \frac{1}{n}\left(\frac{1}{2\pi}\right)^2\sum_{j,k,j\neq k} I_B(0, s'_j, s_j)I_B(0, s'_k, s_k)\prod_{\gamma=1,\gamma\neq j,k}^{n}\delta_{x'_{\gamma}s'_{\gamma},x_{\gamma}s_{\gamma}}. \quad \text{(A47)}$$

In $I_{A2}(0, s'_i, s_i)$, if $s'_i \neq s_i$, $I_{A2}(0, s'_i, s_i) = 0$. Thus the first part in $M_{\xi'\xi}$ is zero if $\xi' \neq \xi$. If $\xi' = \xi$, it takes on the value of $(n-1)(1-\frac{1}{\sqrt{2}})$.

For the second part in $M_{\xi'\xi}$, integrals $I_B(0, \uparrow, \uparrow)$, $I_B(0, \uparrow, \downarrow)$, and $I_B(0, \downarrow, \uparrow)$ are all $i(2-\sqrt{2})\pi$, while $I_B(0, \downarrow, \downarrow) = -i(2-\sqrt{2})\pi$. The values of $I_B(0, s'_j, s_j)I_B(0, s'_k, s_k)$ corresponding to different combinations of s'_j, s'_k, s_j, and s_k are listed in Table I:

(s'_j, s'_k, s_j, s_k)	Value
$(\uparrow,\uparrow,\uparrow,\uparrow)$, $(\uparrow,\uparrow,\uparrow,\downarrow)$, $(\uparrow,\uparrow,\downarrow,\uparrow)$, $(\uparrow,\uparrow,\downarrow,\downarrow)$, $(\uparrow,\downarrow,\uparrow,\uparrow)$, $(\uparrow,\downarrow,\downarrow,\uparrow)$, $(\downarrow,\uparrow,\uparrow,\uparrow)$, $(\downarrow,\uparrow,\uparrow,\downarrow)$, $(\downarrow,\downarrow,\uparrow,\uparrow)$, $(\downarrow,\downarrow,\downarrow,\downarrow)$	$-(2-\sqrt{2})^2\pi^2$
$(\uparrow,\downarrow,\uparrow,\downarrow)$, $(\uparrow,\downarrow,\downarrow,\downarrow)$, $(\downarrow,\uparrow,\downarrow,\uparrow)$, $(\downarrow,\uparrow,\downarrow,\downarrow)$, $(\downarrow,\downarrow,\uparrow,\downarrow)$, $(\downarrow,\downarrow,\downarrow,\uparrow)$	$(2-\sqrt{2})^2\pi^2$

When $\xi' = \xi$, i.e., the left state vector is the same as the right state vector, we denote the number of particles that are spinning up as $n_{\uparrow}$, and those spinning down as $n_{\downarrow}$. Then $n_{\uparrow} + n_{\downarrow} = n$, and

$$\begin{aligned} M_{\xi'\xi} &= (n-1)\left(1-\frac{1}{\sqrt{2}}\right) + \frac{1}{n}\sum_{j\neq k}(-1)^{\delta_{s_j,s_k}}\left(1-\frac{1}{\sqrt{2}}\right)^2 \\ &= (n-1)\left(1-\frac{1}{\sqrt{2}}\right) + \frac{2}{n}\left[-\left(C^2_{n_{\uparrow}} + C^2_{n_{\downarrow}}\right) + n_{\uparrow}n_{\downarrow}\right]\left(1-\frac{1}{\sqrt{2}}\right)^2 \\ &= (n-1)\left(1-\frac{1}{\sqrt{2}}\right) - \frac{1}{n}[(n_{\uparrow}-n_{\downarrow})^2 - n]\left(1-\frac{1}{\sqrt{2}}\right)^2. \end{aligned} \quad \text{(A48)}$$

When $d(\xi', \xi) > 2$, $M_{\xi'\xi} = 0$, and when $d(\xi', \xi) = 1$, there is a mismatch in one of the spins pairs. We denote the number of spinning up pairs in the matched $n-1$ pairs as $n'_{\uparrow}$ and those spinning down as $n'_{\downarrow}$; the matrix elements are

$$M_{\xi'\xi} = \frac{2}{n}[-n'_{\uparrow} + n'_{\downarrow}]\left(1-\frac{1}{\sqrt{2}}\right)^2. \quad \text{(A49)}$$

When $d(\xi', \xi) = 2$,

$$M_{\xi'\xi} = -\frac{2}{n}\left(1-\frac{1}{\sqrt{2}}\right)^2. \quad \text{(A50)}$$

If we rewrite the subscripts of matrix M as i, j, k, then

$$M_{ii} = (n-1)\left(1-\frac{1}{\sqrt{2}}\right) + \frac{1}{n}[n - (2W(i)-n)^2]\left(1-\frac{1}{\sqrt{2}}\right)^2, \quad \text{(A51)}$$

$$M_{jk} = \frac{2}{n}\left(1-\frac{1}{\sqrt{2}}\right)^2[\delta_{d(j,k),1}(n-1-2\min\{W(j), W(k)\}) - \delta_{d(j,k),2}], \ (j\neq k), \quad \text{(A52)}$$

where $i, j, k = 0, 1, 2, \dots, 2^n-1$ and $W(i)$ represents the Hamming weight of integer i, i.e., the number of 1's in the n-bit binary form of integer i. Here $d(j, k)$ represents the Hamming distance between integers j and k, which is the number of bit positions where the corresponding two bits in the binary form of i and j are different. δ is the Kronecker delta.

The maximum and minimum values of c_2 as a function of the initial coin state are the maximum and minimum eigenvalues of M, respectively.

5. Solving eigenvalues and eigenvectors

Given the number of particles, n, the matrix elements of M are

$$M_{ii} =(n-1)\left(1-\frac{1}{\sqrt{2}}\right)+\frac{1}{n}[n-(2W(i)-n)^2]\left(1-\frac{1}{\sqrt{2}}\right)^2$$

$$M_{jk} =\frac{2}{n}\left(1-\frac{1}{\sqrt{2}}\right)^2[\delta_{d(j,k),1}(n-1-2\min\{W(j),W(k)\})-\delta_{d(j,k),2}],\ (j\neq k), \tag{A53}$$

where $i, j, k \in \{0, 1, \dots, 2^n-1\}$. We define

$$B_n=\left(1-\frac{1}{\sqrt{2}}\right)^{-2}\frac{n}{2}M_n-\frac{n(n-1)}{\sqrt{2}}I, \tag{A54}$$

the matrix elements of which are

$$b_{ii}=n(n-1)+\tfrac{1}{2}[n-(2W(i)-n)^2]$$

$$b_{jk}=\delta_{d(j,k),1}(n-1-2\min\{W(j),W(k)\})-\delta_{d(j,k),2},\ (j\neq k). \tag{A55}$$

When $n\geqslant 2$, we define the 2×2 matrix $P_{ij}=(-1)^{c(i,j)}Z^{d(i,j)}$, where

$$Z=\begin{bmatrix}0 & 1\\ 1 & 2\end{bmatrix}, \tag{A56}$$

$i, j \in \{0, 1, \dots, 2^n-1\}$ are even; $c(i, j)$ represents the number of bit positions where the corresponding two bits in the binary form of i and j are all ones.

Theorem 1. Denote i, j to be the row and column locations of the upper-left corner element of the submatrix P_{ij} in the $2^n\times 2^n$ matrix P. The submatrices P_{ij} make up the matrix P_n, such that $P_n^{-1}B_nP_n$ is diagonal matrix $(\mu_k I_2)$, where k is an even number and I_2 is a 2×2 identity matrix.

Proof. When $n=2$,

$$P_n^{-1}B_nP_n=\begin{bmatrix}0&0&0&0\\0&0&0&0\\0&0&4&0\\0&0&0&4\end{bmatrix}. \tag{A57}$$

We prove the theorem by mathematical induction. Assume that it holds true for n. Then for $n+1$, let $B_n=(B_{ij})$ be the 2×2 submatrix partition and similarly $B_{n+1}=(B'_{ij}),\ P_n=(P_{ij}), P_{n+1}=(P'_{ij})$, where i, j are even numbers. It can be proved that $\forall i$, $k<2^{n+1}$, $2|i$, $2|k$, $\exists\mu'$ such that

$$\sum_{\substack{0\leqslant j<2^{n+1}\\ 2|j}}B'_{ij}P'_{jk}=\mu'P'_{ik}. \tag{A58}$$

We first prove it for the case of $i<2^n$, $k<2^n$. Let $j<2^n$,

$$B'_{ij}=B_{ij}+\begin{bmatrix}\delta_{d(i,j),1} & \delta_{d(i,j+1),1}\\ \delta_{d(i,j+1),1} & \delta_{d(i+1,j+1),1}\end{bmatrix}=B_{ij}+\delta_{d(i,j),1}I_2(i\neq j), \tag{A59}$$

$$B'_{ii}=B_{ii}+\begin{bmatrix}n+2W(i) & 1\\ 1 & n+2+2W(i)\end{bmatrix}, \tag{A60}$$

$$B'_{i,j+2^n}=\begin{bmatrix}-\delta_{d(i,j+2^n),2} & -\delta_{d(i,j+2^n+1),2}\\ -\delta_{d(i+1,j+2^n),2} & -\delta_{d(i+1,j+2^n+1),2}\end{bmatrix}=-\delta_{d(i,j),1}I_2(i\neq j), \tag{A61}$$

$$B'_{i,i+2^n}=\begin{bmatrix}n-2W(i) & -1\\ -1 & n-2-2W(i)\end{bmatrix}. \tag{A62}$$

Hence,

$$\sum_{\substack{0\leqslant j<2^{n+1}\\ 2|j}}B'_{ij}P'_{jk}=\sum_{\substack{j<2^n\\ 2|j\neq i}}(B_{ij}+\delta_{d(i,j),1}I)P_{jk}+\left[B_{ii}+\begin{pmatrix}n+2W(i) & 1\\ 1 & n+2+2W(i)\end{pmatrix}\right]P_{ik}$$

$$+\sum_{\substack{j<2^n\\ 2|j\neq i}}[-\delta_{d(i,j),1}ZP_{jk}]+\begin{pmatrix}n-2W(i) & -1\\ -1 & n-2-2W(i)\end{pmatrix}ZP_{ik}. \tag{A63}$$

Utilizing the induction hypothesis, i.e. $\exists\mu$ such that $\sum_{\substack{j<2^n\\ 2|j}} B_{ij}P_{jk}=\mu P_{ik}$, we obtain

$$\sum_{\substack{0\leqslant j<2^{n+1}\\ 2|j}} B'_{ij}P'_{jk}=\sum_{\substack{j<2^n\\ 2|j\neq i}}\delta_{d(i,j),1}P_{jk}(I-Z)+\left[\begin{pmatrix} n+2W(i) & 1\\ 1 & n+2+2W(i)\end{pmatrix}+\begin{pmatrix} n-2W(i) & -1\\ -1 & n-2-2W(i)\end{pmatrix}Z\right]P_{ik}+\mu P_{ik}. \tag{A64}$$

Here we consider $\sum_{\substack{j<2^n\\ 2|j,d(i,j)=1}} P_{jk}P_{ik}^{-1}=rI+yZ$, where $r=2\times\#\{j|(i,k)_{\vartheta(i,j)}=(0,1)\}-2\times\#\{j|(i,k)_{\vartheta(i,j)}=(1,0)\}$, $y=\#\{j|(i,k)_{\vartheta(i,j)}=(0\text{ or }1,0)\}-\#\{j|(i,k)_{\vartheta(i,j)}=(0\text{ or }1,1)\}$. $\#\{j|(i,k)_{\vartheta(i,j)}=(0,1)\}$ represents the number of j's for $0\leqslant j<2^n$, $2|j$, $d(i,j)=1$ such that the binary form of i is 0 and k is 1 on the bit where the binary form of i differs from j. The notation $\vartheta(i,j)$ denotes the bit position where i is different from j. One can deduce that $r=2(W(k)-W(i))$, $y=n-2W(k)-1$. Taking $\mu'=\mu+4W(k)$, it can be verified that Eq. (A64) can be turned into

$$\begin{aligned}\sum_{\substack{0\leqslant j<2^{n+1}\\ 2|j}} B'_{ij}P'_{jk}=&(rI+yZ)(I-Z)P_{ik}+\left[\begin{pmatrix} n+2W(i) & 1\\ 1 & n+2+2W(i)\end{pmatrix}+\begin{pmatrix} n-2W(i) & -1\\ -1 & n-2-2W(i)\end{pmatrix}Z\right]P_{ik}+\mu P_{ik}\\ =&[(rI+yZ)(I-Z)+(n+2W(i)-1)I+(n-2W(i)-1)Z+\mu I]P_{ik}=\mu' P_{ik}=\mu' P'_{ik}.\end{aligned} \tag{A65}$$

Note that P_{ik} commutes with Z.

When $i<2^n$, $k\geqslant 2^n$, we denote $k'=k-2^n$, so $0\leqslant k'<2^n$. Similarly,

$$\begin{aligned}\sum_{\substack{0\leqslant j<2^{n+1}\\ 2|j}} B'_{ij}P'_{jk}=&\sum_{\substack{j<2^n\\ 2|j\neq i}}(B_{ij}+\delta_{d(i,j),1}I)ZP_{jk'}+\left[B_{ii}+\begin{pmatrix} n+2W(i) & 1\\ 1 & n+2+2W(i)\end{pmatrix}\right]ZP_{ik'}\\ &+\sum_{\substack{j<2^n\\ 2|j\neq i}}\delta_{d(i,j),1}P_{jk'}-\begin{pmatrix} n-2W(i) & -1\\ -1 & n-2-2W(i)\end{pmatrix}P_{ik'}.\end{aligned} \tag{A66}$$

Hence, taking $\mu'=4n-4W(k')+\mu$, we obtain

$$\begin{aligned}\sum_{\substack{0\leqslant j<2^{n+1}\\ 2|j}} B'_{ij}P'_{jk}=&(rI+yZ)(Z+I)P_{ik'}+\left[\begin{pmatrix} n+2W(i) & 1\\ 1 & n+2+2W(i)\end{pmatrix}Z-\begin{pmatrix} n-2W(i) & -1\\ -1 & n-2-2W(i)\end{pmatrix}\right]P_{ik'}+\mu ZP_{ik'}\\ =&[4(n-W(k'))+\mu]P'_{ik}=\mu' P'_{ik}.\end{aligned} \tag{A67}$$

When $i\geqslant 2^n$, $k<2^n$, we let $j<2^n$ and $i'=i-2^n$,

$$B'_{i'+2^n,j}=B'_{j,i'+2^n}=\begin{pmatrix} -\delta_{d(j,i'+2^n),2} & -\delta_{d(j,i'+2^n+1),2}\\ -\delta_{d(j+1,i'+2^n),2} & -\delta_{d(j+1,i'+2^n+1),2}\end{pmatrix}=-\delta_{d(i',j),1}I_2(i'\neq j), \tag{A68}$$

$$B'_{i'+2^n,i'}=\begin{pmatrix} n-2W(i') & -1\\ -1 & n-2-2W(i')\end{pmatrix}, \tag{A69}$$

$$B'_{i'+2^n,j+2^n}=\begin{pmatrix} -2\delta_{d(i',j),1} & -2\delta_{d(i',j+1),1}\\ -2\delta_{d(i'+1,j),1} & -2\delta_{d(i'+1,j+1),1}\end{pmatrix}+B'_{i'j}=B_{i'j}-\delta_{d(i',j),1}I_2(i'\neq j), \tag{A70}$$

$$B'_{i'+2^n,i'+2^n}=\begin{pmatrix} -4W(i')+2n & -2\\ -2 & -4-4W(i')+2n\end{pmatrix}+B'_{i'i'}=B_{i'i'}+\begin{pmatrix} 3n-2W(i') & -1\\ -1 & 3n-2W(i')-2\end{pmatrix}. \tag{A71}$$

It can also be deduced that

$$\begin{aligned}\sum_{\substack{0\leqslant j<2^{n+1}\\ 2|j}} B'_{i'+2^n,j}P'_{jk}=&\sum_{\substack{j<2^n\\ 2|j\neq i'}}(-\delta_{d(i',j),1})P_{jk}+\begin{pmatrix} n-2W(i') & -1\\ -1 & n-2-2W(i')\end{pmatrix}P_{i'k}\\ &+\sum_{\substack{j<2^n\\ 2|j\neq i'}}(B_{i'j}-\delta_{d(i',j),1})ZP_{jk}+\left[B_{i'i'}+\begin{pmatrix} 3n-2W(i') & -1\\ -1 & 3n-2W(i')-2\end{pmatrix}\right]ZP_{i'k}\\ =&[4W(k)+\mu]P'_{i,k}.\end{aligned} \tag{A72}$$

When $i \geqslant 2^n$, $k \geqslant 2^n$, we let $k' = k - 2^n$, $i' = i - 2^n$. Then

$$\begin{aligned}\sum_{\substack{0\leqslant j<2^{n+1}\\2|j}} B'_{i'+2^n,j}P'_{j,k'+2^n} &= \sum_{\substack{j<2^n\\2|j\neq i'}}(-\delta_{d(i',j),1})ZP_{jk'} + \begin{pmatrix} n-2W(i') & -1\\ -1 & n-2-2W(i')\end{pmatrix}ZP_{i'k'}\\ &\quad -\sum_{\substack{j<2^n\\2|j\neq i'}}(B_{i'j}-\delta_{d(i',j),1})P_{jk'} - \left[B_{i'i'} + \begin{pmatrix} 3n-2W(i') & -1\\ -1 & 3n-2W(i')-2\end{pmatrix}\right]P_{i'k'}\\ &= [4n-4W(k')+\mu]P'_{i,k}. \end{aligned} \tag{A73}$$

■

According to Theorem 1, the eigenvalue corresponding to the column subscript k is

$$\mu_k^n = \begin{cases} \mu_k^{n-1} + 4W(k), & 0 \leqslant k < 2^{n-1}\\ 4(n-1) - 4W(k-2^{n-1}) + \mu_{k-2^{n-1}}^{n-1}, & 2^{n-1} \leqslant k < 2^n, \end{cases} \tag{A74}$$

where k is an even number. As $\mu_0^2 = 0$ and $\mu_2^2 = 4$, for n particles, we have

$$\mu_k = 4W(k)W(2^n - 1 - k). \tag{A75}$$

Each μ_k ($0 \leqslant k < 2^n$, $2|k$) corresponds to two eigenvectors, and the corresponding eigenvalue of M_n is $\eta_k = (1 - \frac{1}{\sqrt{2}})^2[\frac{2\mu_k}{n} + (n-1)\sqrt{2}]$. By the range of k, it can be inferred that $0 \leqslant W(k) \leqslant n-1$, $W(k) \in \mathbb{Z}$, and there are $C_{n-1}^{W(k)}$ different k's that correspond to the same value of $W(k)$. Note that for different k's, e.g., k and k', η_k and $\eta_{k'}$ are the same when $W(k) = n - W(k')$, which should be taken into account in counting the degeneracies of the eigenvalues. We assume that $k, k' \in \{0, 2, 4, \dots, 2^n - 2\}$. When $W(k) = 0$, there is no k' satisfying $W(k') = n - W(k) = n$. When n is odd, for any given k satisfying $1 \leqslant W(k) \leqslant (n-1)/2$, there are k''s ($k' \neq k$) such that $(n+1)/2 \leqslant W(k') \leqslant n-1$ and $W(k') = n - W(k)$. When n is even, for any given k satisfying $1 \leqslant W(k) \leqslant n/2 - 1$, there is another set of k''s ($k' \neq k$) such that $n/2 + 1 \leqslant W(k') \leqslant n-1$ and $W(k') = n - W(k)$, and for those k's satisfying $W(k) = n/2$, as $n - W(k) = W(k)$, the degeneracy of η_k is $2C_{n-1}^{W(k)}$. So we arrive at the following result for the degeneracy of η_k:

$$\text{count}(\eta_k) = \begin{cases} 2, & k = 0\\ 2\left(C_{n-1}^{W(k)} + C_{n-1}^{n-W(k)}\right), & k \neq 0, n \text{ is odd}\\ 2\left(C_{n-1}^{W(k)} + C_{n-1}^{n-W(k)}\right), & k \neq 0, W(k) \neq \frac{n}{2}, n \text{ is even}\\ 2C_{n-1}^{W(k)}, & W(k) = \frac{n}{2}, n \text{ is even.} \end{cases} \tag{A76}$$

6. Proof of partial exchange symmetry

Using the relation $Z^2 = 2Z + I$, it can be proven that

$$Z^\alpha = \begin{bmatrix} F(\alpha-1) & F(\alpha)\\ F(\alpha) & F(\alpha+1)\end{bmatrix}, \tag{A77}$$

where $\alpha \in \mathbb{Z}$ and

$$F(\alpha) = \frac{(1+\sqrt{2})^\alpha - (1-\sqrt{2})^\alpha}{2\sqrt{2}}. \tag{A78}$$

$F(\alpha) \geqslant 0$ when $\alpha \geqslant -1$. So,

$$\begin{aligned} P_{ij} &= (-1)^{c(i,j)}Z^{d(i,j)}\\ &= (-1)^{c(i,j)}\begin{bmatrix} F(d(i,j)-1) & F(d(i,j))\\ F(d(i,j)) & F(d(i,j)+1)\end{bmatrix}. \end{aligned} \tag{A79}$$

To analyze the exchange symmetry, we take a close look at the binary form of subscripts i and j, that $i, j \in \{0, 2, \dots, 2^n - 2\}$. Each column of the matrix $P_n = (P_{ij})$ is an unnormalized eigenvector of matrix M. Combining the normalized eigenvectors and the position state, we obtain the optimized initial states for the quantum walk. Let $i', j' \in \{0, 1, \dots, 2^n - 1\}$ be the row and column subscripts of the matrix element $p_{i'j'}$ in P_n. Then the element in row $i' = (i'_1 i'_2 \cdots i'_n)_2$ of a normalized eigenvector is the coefficient with respect to the product basis $|i'\rangle = |i'_1\rangle|i'_2\rangle\cdots|i'_n\rangle$, where $|i'_\beta\rangle$ corresponds to the βth particle. Let P_{ij} be the 2×2 submatrix of P_n that the matrix element $p_{i'j'}$ belongs to, and the row and column locations of the upper-left element of P_{ij} are $i = 2\lfloor i'/2\rfloor$, $j = 2\lfloor j'/2\rfloor$. We will see that each eigenstate is invariant under the permutation of some of the n particles, and we define this invariance of the eigenstates as *partial exchange symmetry*. When the uth and u'th particles are swapped, the state vector is changed by exchanging the single-particle states of the uth and u'th particles in all the product bases that compose the whole multiparticle state.

Consider an initial state with the coin state corresponding to the j'th column of matrix P_n as

$$|\Psi^{(j')}\rangle = |00\cdots 0\rangle \otimes \sum_{i'} a_{i'}^{(j')}|i'\rangle, \tag{A80}$$

where $|i'\rangle = |i'_1 i'_2 \cdots i'_n\rangle$, and $a_{i'}^{(j')} = p_{i'j'}/\sqrt{\sum_{i''}|p_{i''j'}|^2}$. We define a map $g_{\beta,\gamma} : \{0, 1, \dots, 2^n - 1\} \to \{0, 1, \dots, 2^n - 1\}$ that maps a number to another whose numbers on bit positions β and γ of the binary representation are swapped, e.g., $g_{\beta,\gamma}((i_1\cdots i_\beta\cdots i_\gamma\cdots i_n)_2)=(i_1\cdots i_\gamma\cdots i_\beta\cdots i_n)_2$. Since the initial position states of the particles are all $|0\rangle$, the symmetry of the state $|\Psi^{(j')}\rangle$ is completely determined by its multiparticle coin state. Then the invariance of the state with respect to exchanging the βth and γth particles is equivalent to $\sum_{i'} a_{i'}^{(j')}|i'\rangle=\sum_{i'} a_{i'}^{(j')}|g_{\beta,\gamma}(i')\rangle$, i.e., $a_{i'}^{(j')}=a_{g_{\beta,\gamma}(i')}^{(j')}$ and thus $p_{i'j'}=p_{g_{\beta,\gamma}(i'),j'}$ for all i'. We define another map $h_{\beta,\gamma}:\{0,1,\dots,2^n-1\}\to\{0,2,\dots,2^n-2\}$, such that $h_{\beta,\gamma}(i')=2\lfloor g_{\beta,\gamma}(i')/2\rfloor$. Then $h_{\beta,\gamma}(i')$ is the row subscript of the upper-left corner of the submatrix that the matrix element $p_{i'j'}$ is mapped to by exchanging particles β and γ. We will omit the subscripts β and γ in $g_{\beta,\gamma}$ and $h_{\beta,\gamma}$ for simplicity in the following proof.

Lemma 1. If a swap in the binary form of i' occurs between two of the first $n-1$ bits where the corresponding bits in j are both 0 or 1, then $c(i,j)$ and $d(i,j)$ are unchanged for all i', i.e., $c(h(i'),j)=c(i,j)$, $d(h(i'),j)=d(i,j)$.

Lemma 2. If a swap in the binary form of i' occurs between two of the first $n-1$ bits where the corresponding bits in j are 1 and 0, respectively, there always exists an i' such that both $c(i,j)$ and $d(i,j)$ are changed, i.e., $c(h(i'),j)\neq c(i,j)$ and $d(h(i'),j)\neq d(i,j)$.

Lemma 3. When a swap occurs between two of the first $n-1$ particles, the state is unchanged if and only if the particles corresponding to the bit positions where the bits in j are both 0 or 1 are swapped, as in the way described in Lemma 1.

Proof. The sufficiency is evident. The following is the proof of necessity. If one does not perform the swap as described in Lemma 1, but performs a swap as described in Lemma 2 that the two particles to be swapped correspond to the bit positions where the bits in j are 0 and 1, respectively, there exists an i', such that $c(h(i'),j)=c(i,j)\pm1$ and $d(h(i'),j)=d(i,j)\pm2$, so the element $p_{g(i'),j'}$ in the submatrix $P_{h(i'),j}=(-1)^{c(h(i'),j)}Z^{d(h(i'),j)}$ that $p_{i'j'}$ is mapped to would be different from $p_{i'j'}$. Specifically, if i' is equal to j on the two bit positions to be swapped, respectively, then $c(h(i'),j)=c(i,j)-1$ and $d(h(i'),j)=d(i,j)+2$, and if i' is different from j on both of the two bit positions to be swapped, then $c(h(i'),j)=c(i,j)+1$ and $d(h(i'),j)=d(i,j)-2$. As $d(h(i'),j)\geqslant0$, all of the elements in matrix $Z^{d(h(i'),j)}$ are greater than or equal to zero. So $p_{i'j'}$ and $p_{g(i'),j'}$ would be at least different in sign due to the change of $c(i,j)$ into $c(h(i'),j)$ in these situations, except for those i''s such that $p_{i'j'}=0$. But it can be proven that $p_{g(i'),j'}$ must be nonzero if $p_{i'j'}=0$. To conclude, if $j_\beta\neq j_\gamma$, $1\leqslant\beta,\gamma\leqslant n-1$, $\exists i'$ such that $p_{i'j'}\neq p_{g_{\beta,\gamma}(i'),j'}$, so the state is changed. ■

Lemma 4. When swapping the particle corresponding to the last bit with the one corresponding to one of the first $n-1$ bits, the state is unchanged if and only if the particle corresponding to the last bit is swapped with the particle corresponding to the bit position where the corresponding bit in j is 0.

Proof of sufficiency. If the particle corresponding to the last bit is swapped with the particle corresponding to one of the first $n-1$ bit positions where the corresponding bit in j is 0, i.e., we swap the βth and γth particles such that $\beta=n$, $1\leqslant\gamma\leqslant n-1$, $j_\gamma=0$, we will show that the coefficients of all of the bases remain unchanged after the swap, i.e., $a_{i'}^{(j')}=a_{g_{\beta,\gamma}(i')}^{(j')}$.

As $j_\gamma=0$, $c(h(i'),j)=c(i,j)$ holds true for all $i'\in\{0,1,\dots,2^n-1\}$. For each i' with $i'_\beta=i'_n=0$, if i'_γ is 0, the swap does not change i'; i.e., the corresponding basis is unchanged. But if i'_γ is 1, $d(h(i'),j)=d(i,j)-1$, and the corresponding submatrix where $p_{g(i'),j'}$ locates is

$$\begin{aligned}P_{h(i'),j}&=(-1)^{c(i,j)}Z^{d(i,j)-1}\\&=(-1)^{c(i,j)}\begin{bmatrix}F(d(i,j)-2)&F(d(i,j)-1)\\F(d(i,j)-1)&F(d(i,j))\end{bmatrix},\end{aligned}\tag{A81}$$

while the original submatrix P_{ij} where the matrix element $p_{i'j'}$ locates is given by

$$P_{ij}=(-1)^{c(i,j)}\begin{bmatrix}F(d(i,j)-1)&F(d(i,j))\\F(d(i,j))&F(d(i,j)+1)\end{bmatrix}.\tag{A82}$$

We can see that the first row of P_{ij} where $p_{i'j'}$ locates is identical to the second row of $P_{h(i'),j}$ where $p_{g(i'),j'}$ locates, so if we modify a basis where the last bit is $i'_n=0$, it is mapped to another basis in which the coefficient is the same as that in the original basis, i.e., $p_{i',j'}=p_{g(i'),j'}$ for all i' with $i'_n=0$.

For each i' with $i'_n=1$, the basis is unchanged if the bit i'_γ which is swapped with i'_n is 1. If the bit i'_γ is 0, then $d(h(i'),j)=d(i,j)+1$,

$$P_{h(i'),j}=(-1)^{c(i,j)}\begin{bmatrix}F(d(i,j))&F(d(i,j)+1)\\F(d(i,j)+1)&F(d(i,j)+2)\end{bmatrix}.\tag{A83}$$

The second row of P_{ij} is the same as the first row of $P_{h(i'),j}$, hence $p_{i'j'}=p_{g(i'),j'}$.

Proof of necessity. If the particle corresponding to the last bit is swapped with the particle corresponding to one of the first $n-1$ bit positions where the corresponding bit in j is 1, i.e., swapping the βth and γth particles such that $\beta=n$, $1\leqslant\gamma\leqslant n-1$, $j_\gamma=1$, there always exists i' such that $c(h(i'),j)=c(i,j)-1$ and $d(h(i'),j)=d(i,j)+1$ when $i'_n=0$ and $i'_\gamma=1$, or reversely $c(h(i'),j)=c(i,j)+1$ and $d(h(i'),j)=d(i,j)-1$ when $i'_n=1$ and $i'_\gamma=0$. So the corresponding $p_{i'j'}$ and $p_{g(i'),j'}$ are at least different in sign due to the change of $c(i,j)$ into $c(h(i'),j)$ after the swap, except for those i''s such that $p_{i'j'}=0$, similar to the situation discussed in the proof of Lemma 3. By comparing the first row of P_{ij} with the second row of $P_{h(i'),j}$ when $i'_n=0$, $i'_\gamma=1$ and comparing the second row of P_{ij} with the first row of $P_{h(i'),j}$ when $i'_n=1$, $i'_\gamma=0$, we can also prove that $p_{i'j'}$ and $p_{g(i'),j'}$ cannot be simultaneously 0. Thus the state is changed if the particle corresponding to the last bit position is swapped with the particle corresponding to the bit position where the corresponding bit in j is 1. ■

Based on Lemmas 1–4, we are led to the following theorem.

Theorem 2. Given an initial state $|\Psi^{(j')}\rangle$, the state is unchanged if and only if the swap happens among some of the first $n-1$ particles where the corresponding bits in $j=2\lfloor j'/2\rfloor$ are all 1 or 0, or between the last particle and one of the first $n-1$ particles where the corresponding bit in j is 0.

So we can group the particles whose corresponding bits in j are 1 into a set and the other particles into another.

Then we connect each pair of particles with an undirected edge if the state is unchanged after they are swapped. Each of the two subsets (when $j \neq 0$) of particles makes up a complete graph. If we denote $n_\uparrow$ and $n_\downarrow$ as the number of 1's and 0's in the binary form of j, respectively (j is even), the number of possible ways to exchange two particles preserving an eigenstate is $p_j = \frac{n_\uparrow(n_\uparrow-1)}{2} + \frac{n_\downarrow(n_\downarrow-1)}{2}$, $n_\uparrow + n_\downarrow = n$, and the two disconnected complete subgraphs have $n_\uparrow$ and $n_\downarrow$ vertices, respectively. We can rewrite this using the Hamming weight, $p_j = \frac{W(j)(W(j)-1)}{2} + \frac{(n-W(j))(n-W(j)-1)}{2} = W(j)^2 - nW(j) + C_n^2$, so $\eta_j = (1-1/\sqrt{2})^2[8(C_n^2 - p_j)/n + (n-1)\sqrt{2}]$. When $j=0$, all the bits in j are 0, so there is only one complete graph and all of the particles are vertices of this graph. As the evolution operator $\hat{U}_n$ is symmetric with respect to particles, the symmetry of the state is preserved during the evolution.

7. Entanglement between complete graphs

Since the particles in each of the two complete graphs possess exchange symmetry, for simplicity, the eigenstates can be represented by the superpositions of direct products of bosonic Fock states. When k is an even number, the kth eigenstate is

$$\begin{aligned}|\eta_k\rangle =& C \sum_{\substack{0\leqslant w_1\leqslant W(k)\\0\leqslant w_0\leqslant n-W(k)}} (-1)^{w_1} F(W(k)-w_1+w_0-1)\sqrt{\frac{(n-W(k))!}{w_0!(n-W(k)-w_0)!}}\sqrt{\frac{W(k)!}{w_1!(W(k)-w_1)!}}\\ &\times |1_{w_0}0_{n-W(k)-w_0}\rangle \otimes |1_{w_1}0_{W(k)-w_1}\rangle\\ =& C\Bigg[\frac{(1+\sqrt{2})^{W(k)-1}}{2\sqrt{2}} \sum_{0\leqslant w_0\leqslant n-W(k)} (1+\sqrt{2})^{w_0}\sqrt{\frac{(n-W(k))!}{w_0!(n-W(k)-w_0)!}}|1_{w_0}0_{n-W(k)-w_0}\rangle\\ &\otimes \sum_{0\leqslant w_1\leqslant W(k)} (-1)^{w_1}(1+\sqrt{2})^{-w_1}\sqrt{\frac{W(k)!}{w_1!(W(k)-w_1)!}}|1_{w_1}0_{W(k)-w_1}\rangle\\ &-\frac{(1-\sqrt{2})^{W(k)-1}}{2\sqrt{2}} \sum_{0\leqslant w_0\leqslant n-W(k)} (1-\sqrt{2})^{w_0}\sqrt{\frac{(n-W(k))!}{w_0!(n-W(k)-w_0)!}}|1_{w_0}0_{n-W(k)-w_0}\rangle\\ &\otimes \sum_{0\leqslant w_1\leqslant W(k)} (-1)^{w_1}(1-\sqrt{2})^{-w_1}\sqrt{\frac{W(k)!}{w_1!(W(k)-w_1)!}}|1_{w_1}0_{W(k)-w_1}\rangle\Bigg], \end{aligned} \tag{A84}$$

where $\{|1_{w_0}0_{n-W(k)-w_0}\rangle | 0 \leqslant w_0 \leqslant n-W(k)\}$ and $\{|1_{w_1}0_{W(k)-w_1}\rangle | 0 \leqslant w_1 \leqslant W(k)\}$ are two sets of orthonormal vectors. C is the normalization factor.

We denote

$$|\tilde{\varphi}_A^1\rangle \equiv \sum_{0\leqslant w_0\leqslant n-W(k)} (1+\sqrt{2})^{w_0}\sqrt{\frac{(n-W(k))!}{w_0!(n-W(k)-w_0)!}}|1_{w_0}0_{n-W(k)-w_0}\rangle, \tag{A85}$$

$$|\tilde{\varphi}_B^1\rangle \equiv \sum_{0\leqslant w_1\leqslant W(k)} (-1)^{w_1}(1+\sqrt{2})^{-w_1}\sqrt{\frac{W(k)!}{w_1!(W(k)-w_1)!}}|1_{w_1}0_{W(k)-w_1}\rangle, \tag{A86}$$

$$|\tilde{\varphi}_A^2\rangle \equiv \sum_{0\leqslant w_0\leqslant n-W(k)} (1-\sqrt{2})^{w_0}\sqrt{\frac{(n-W(k))!}{w_0!(n-W(k)-w_0)!}}|1_{w_0}0_{n-W(k)-w_0}\rangle, \tag{A87}$$

$$|\tilde{\varphi}_B^2\rangle \equiv \sum_{0\leqslant w_1\leqslant W(k)} (-1)^{w_1}(1-\sqrt{2})^{-w_1}\sqrt{\frac{W(k)!}{w_1!(W(k)-w_1)!}}|1_{w_1}0_{W(k)-w_1}\rangle, \tag{A88}$$

and normalize them using the following equations:

$$\sum_{0\leqslant w_0\leqslant n-W(k)} (1+\sqrt{2})^{2w_0} C_{n-W(k)}^{w_0} = (4+2\sqrt{2})^{n-W(k)}, \tag{A89}$$

$$\sum_{0\leqslant w_1\leqslant W(k)} (1+\sqrt{2})^{-2w_1} C_{W(k)}^{w_1} = (4-2\sqrt{2})^{W(k)}. \tag{A90}$$

We remove the tilde notations for the normalized vectors, and the eigenstate turns into

$$|\eta_k\rangle = C\left[\frac{(1+\sqrt{2})^{W(k)-1}}{2\sqrt{2}}\sqrt{(4+2\sqrt{2})^{n-W(k)}}|\varphi_A^1\rangle \otimes \sqrt{(4-2\sqrt{2})^{W(k)}}|\varphi_B^1\rangle - \frac{(1-\sqrt{2})^{W(k)-1}}{2\sqrt{2}}\sqrt{(4-2\sqrt{2})^{n-W(k)}}|\varphi_A^2\rangle \otimes \sqrt{(4+2\sqrt{2})^{W(k)}}|\varphi_B^2\rangle\right]. \tag{A91}$$

The density matrix of part A is

$$\begin{aligned}\rho_A = \rho_\uparrow &= \mathrm{tr_B}(|\eta_k\rangle\langle\eta_k|)\\ &= |\varphi_A^1\rangle\langle\varphi_A^1|C^2\frac{(1+\sqrt{2})^{2(W(k)-1)}}{8}(4+2\sqrt{2})^{n-W(k)}(4-2\sqrt{2})^{W(k)}\\ &\quad + |\varphi_A^2\rangle\langle\varphi_A^2|C^2\frac{(1-\sqrt{2})^{2(W(k)-1)}}{8}(4-2\sqrt{2})^{n-W(k)}(4+2\sqrt{2})^{W(k)},\end{aligned} \tag{A92}$$

where $\langle\tilde{\varphi}_A^1|\tilde{\varphi}_A^2\rangle = \sum_{0\leqslant w_0\leqslant n-W(k)}(-1)^{w_0}C_{n-W(k)}^{w_0} = 0$ and $C^2 = \{2^{-3+n}(\sqrt{2}-1)^2[(2+\sqrt{2})^n + 4(2-\sqrt{2})^{n-4}]\}^{-1}$.

Finally, we obtain

$$\begin{aligned}\rho_\uparrow = \rho_A &= |\varphi_A^1\rangle\langle\varphi_A^1|[1+(3-2\sqrt{2})^n(17+12\sqrt{2})]^{-1} + |\varphi_A^2\rangle\langle\varphi_A^2|[1+(3+2\sqrt{2})^n/(17+12\sqrt{2})]^{-1}\\ &= |\varphi_A^1\rangle\langle\varphi_A^1|[1+(3-2\sqrt{2})^{n-2}]^{-1} + |\varphi_A^2\rangle\langle\varphi_A^2|[1+(3+2\sqrt{2})^{n-2}]^{-1}.\end{aligned} \tag{A93}$$

So the von Neumann entropy is given by

$$S(\rho_\uparrow) = -\sum_{i=1,2}\nu_i\log\nu_i, \tag{A94}$$

in which $\nu_1 = [1+(3-2\sqrt{2})^{n-2}]^{-1}$, $\nu_2 = [1+(3+2\sqrt{2})^{n-2}]^{-1}$.

Similarly, for the $(k+1)$th eigenstate (k is even),

$$|\eta_{k+1}\rangle = C\sum_{\substack{0\leqslant w_1\leqslant W(k)\\ 0\leqslant w_0\leqslant n-W(k)}}(-1)^{w_1}F(W(k)-w_1+w_0)\sqrt{\frac{(n-W(k))!}{w_0!(n-W(k)-w_0)!}}\sqrt{\frac{W(k)!}{w_1!(W(k)-w_1)!}} \times |1_{w_0}0_{n-W(k)-w_0}\rangle\otimes|1_{w_1}0_{W(k)-w_1}\rangle, \tag{A95}$$

where $C^2 = \{\frac{1}{8}((4-2\sqrt{2})^n + 2^n(2+\sqrt{2})^n)\}^{-1}$. The density matrix of part A is

$$\begin{aligned}\rho_A = \rho_\uparrow &= \mathrm{tr_B}(|\eta_{k+1}\rangle\langle\eta_{k+1}|)\\ &= |\varphi_A^1\rangle\langle\varphi_A^1|C^2\frac{(1+\sqrt{2})^{2W(k)}}{8}(4+2\sqrt{2})^{n-W(k)}(4-2\sqrt{2})^{W(k)}\\ &\quad + |\varphi_A^2\rangle\langle\varphi_A^2|C^2\frac{(1-\sqrt{2})^{2W(k)}}{8}(4-2\sqrt{2})^{n-W(k)}(4+2\sqrt{2})^{W(k)}\\ &= |\varphi_A^1\rangle\langle\varphi_A^1|[1+(3-2\sqrt{2})^n]^{-1} + |\varphi_A^2\rangle\langle\varphi_A^2|[1+(3+2\sqrt{2})^n]^{-1}.\end{aligned} \tag{A96}$$

So in Eq. (A94), $\nu_1 = [1+(3-2\sqrt{2})^n]^{-1}$, $\nu_2 = [1+(3+2\sqrt{2})^n]^{-1}$.

[1] N. Konno, Quantum random walks in one dimension, Quantum Inf. Process. **1**, 345 (2002).

[2] A. M. Childs, R. Cleve, E. Deotto, E. Farhi, S. Gutmann, and D. A. Spielman, Exponential algorithmic speedup by quantum walk, in *Proceedings of the Thirty-Fifth Annual ACM Symposium on Theory of Computing* (Association for Computing Machinery, New York, 2003), pp. 59–68.

[3] H. Tang, C. Di Franco, Z.-Y. Shi, T.-S. He, Z. Feng, J. Gao, K. Sun, Z.-M. Li, Z.-Q. Jiao, T.-Y. Wang, M. S. Kim, and X.-M. Jin, Experimental quantum fast hitting on hexagonal graphs, Nat. Photon. **12**, 754 (2018).

[4] S. E. Venegas-Andraca, Quantum walks: A comprehensive review, Quantum Inf. Process. **11**, 1015 (2012).

[5] K. Kadian, S. Garhwal, and A. Kumar, Quantum walk and its application domains: A systematic review, Comput. Sci. Rev. **41**, 100419 (2021).

[6] R. Portugal, *Quantum Walks and Search Algorithms* (Springer, New York, 2013).

[7] T. G. Wong, L. Tarrataca, and N. Nahimov, Laplacian versus adjacency matrix in quantum walk search, Quantum Inf. Process. **15**, 4029 (2016).

[8] N. Shenvi, J. Kempe, and K. Birgitta Whaley, Quantum random-walk search algorithm, Phys. Rev. A **67**, 052307 (2003).

[9] K. Rudinger, J. K. Gamble, M. Wellons, E. Bach, M. Friesen, R. Joynt, and S. N. Coppersmith, Noninteracting multiparticle quantum random walks applied to the graph isomorphism problem for strongly regular graphs, Phys. Rev. A **86**, 022334 (2012).

[10] B. L. Douglas and J. B. Wang, A classical approach to the graph isomorphism problem using quantum walks, J. Phys. A: Math. Theor. **41**, 075303 (2008).

[11] J. K. Gamble, M. Friesen, D. Zhou, R. Joynt, and S. N. Coppersmith, Two-particle quantum walks applied to the graph isomorphism problem, Phys. Rev. A **81**, 052313 (2010).

[12] S. D. Berry and J. B. Wang, Two-particle quantum walks: Entanglement and graph isomorphism testing, Phys. Rev. A **83**, 042317 (2011).

[13] A. M. Childs, D. Gosset, and Z. Webb, Universal computation by multiparticle quantum walk, Science **339**, 791 (2013).

[14] S. Singh, P. Chawla, A. Sarkar, and C. M. Chandrashekar, Universal quantum computing using single-particle discrete-time quantum walk, Sci. Rep. **11**, 11551 (2021).

[15] A. M. Childs, Universal computation by quantum walk, Phys. Rev. Lett. **102**, 180501 (2009).

[16] Y.-G. Yan, S.-N. Cao, W.-F. Cao, D. Li, Y.-H. Zhou, and W.-M. Shi, Generalized teleportation by means of discrete-time quantum walks on N-lines and N-cycles, Mod. Phys. Lett. B **33**, 1950070 (2019).

[17] H.-J. Li, X.-B. Chen, Y.-L. Wang, Y.-Y. Hou, and J. Li, A new kind of flexible quantum teleportation of an arbitrary multi-qubit state by multi-walker quantum walks, Quantum Inf. Process. **18**, 266 (2019).

[18] P. W. Anderson, Absence of diffusion in certain random lattices, Phys. Rev. **109**, 1492 (1958).

[19] A. Crespi, R. Osellame, R. Ramponi, V. Giovannetti, R. Fazio, L. Sansoni, F. De Nicola, F. Sciarrino, and P. Mataloni, Anderson localization of entangled photons in an integrated quantum walk, Nat. Photon. **7**, 322 (2013).

[20] C. V. C. Mendes, G. M. A. Almeida, M. L. Lyra, and F. A. B. F. de Moura, Localization-delocalization transition in discrete-time quantum walks with long-range correlated disorder, Phys. Rev. E **99**, 022117 (2019).

[21] Y. Shikano and H. Katsura, Localization and fractality in inhomogeneous quantum walks with self-duality, Phys. Rev. E **82**, 031122 (2010).

[22] N. Konno, Localization of an inhomogeneous discrete-time quantum walk on the line, Quantum Inf. Process. **9**, 405 (2010).

[23] N. Inui and N. Konno, Localization of multi-state quantum walk in one dimension, Physica A **353**, 133 (2005).

[24] N. Inui, Y. Konishi, and N. Konno, Localization of two-dimensional quantum walks, Phys. Rev. A **69**, 052323 (2004).

[25] Q. Lin, T. Li, L. Xiao, K. Wang, W. Yi, and P. Xue, Observation of non-Hermitian topological Anderson insulator in quantum dynamics, Nat. Commun. **13**, 3229 (2022).

[26] K. Manouchehri and J. Wang, *Physical Implementation of Quantum Walks* (Springer, Berlin, 2014).

[27] M. Gong, S. Wang, C. Zha, M.-C. Chen, H.-L. Huang, Y. Wu, Q. Zhu, Y. Zhao, S. Li, S. Guo, H. Qian, Y. Ye, F. Chen, C. Ying, J. Yu, D. Fan, D. Wu, H. Su, H. Deng, H. Rong *et al.*, Quantum walks on a programmable two-dimensional 62-qubit superconducting processor, Science **372**, 948 (2021).

[28] Z. Yan, Y.-R. Zhang, M. Gong, Y. Wu, Y. Zheng, S. Li, C. Wang, F. Liang, J. Lin, Y. Xu, C. Guo, L. Sun, C.-Z. Peng, K. Xia, H. Deng, H. Rong, J. Q. You, F. Nori, H. Fan, X. Zhu, and J.-W. Pan, Strongly correlated quantum walks with a 12-qubit superconducting processor, Science **364**, 753 (2019).

[29] P. M. Preiss, R. Ma, M. E. Tai, A. Lukin, M. Rispoli, P. Zupancic, Y. Lahini, R. Islam, and M. Greiner, Strongly correlated quantum walks in optical lattices, Science **347**, 1229 (2015).

[30] A. Schreiber, K. N. Cassemiro, V. Potoček, A. Gábris, P. J. Mosley, E. Andersson, I. Jex, and C. Silberhorn, Photons walking the line: A quantum walk with adjustable coin operations, Phys. Rev. Lett. **104**, 050502 (2010).

[31] M. A. Broome, A. Fedrizzi, B. P. Lanyon, I. Kassal, A. Aspuru-Guzik, and A. G. White, Discrete single-photon quantum walks with tunable decoherence, Phys. Rev. Lett. **104**, 153602 (2010).

[32] A. Schreiber, K. N. Cassemiro, V. Potoček, A. Gábris, I. Jex, and C. Silberhorn, Decoherence and disorder in quantum walks: From ballistic spread to localization, Phys. Rev. Lett. **106**, 180403 (2011).

[33] A. Aspuru-Guzik and P. Walther, Photonic quantum simulators, Nat. Phys. **8**, 285 (2012).

[34] A. Peruzzo, M. Lobino, J. C. F. Matthews, N. Matsuda, A. Politi, K. Poulios, X.-Q. Zhou, Y. Lahini, N. Ismail, K. Worhoff, Y. Bromberg, Y. Silberberg, M. G. Thompson, and J. L. O'Brien, Quantum walks of correlated photons, Science **329**, 1500 (2010).

[35] A. Schreiber, A. Gábris, P. P. Rohde, K. Laiho, M. Štefaňák, V. Potoček, C. Hamilton, I. Jex, and C. Silberhorn, A 2d quantum walk simulation of two-particle dynamics, Science **336**, 55 (2012).

[36] H. Tang, X.-F. Lin, Z. Feng, J.-Y. Chen, J. Gao, K. Sun, C.-Y. Wang, P.-C. Lai, X.-Y. Xu, Y. Wang, L.-F. Qiao, A.-L. Yang, and X.-M. Jin, Experimental two-dimensional quantum walk on a photonic chip, Sci. Adv. **4**, eaat3174 (2018).

[37] F. Cardano, F. Massa, H. Qassim, E. Karimi, S. Slussarenko, D. Paparo, C. de Lisio, F. Sciarrino, E. Santamato, R. W. Boyd, and L. Marrucci, Quantum walks and wavepacket dynamics on a lattice with twisted photons, Sci. Adv. **1**, e1500087 (2015).

[38] H. Defienne, M. Barbieri, I. A. Walmsley, B. J. Smith, and S. Gigan, Two-photon quantum walk in a multimode fiber, Sci. Adv. **2**, e1501054 (2016).

[39] X. Qiang, T. Loke, A. Montanaro, K. Aungskunsiri, X. Zhou, J. L. O'Brien, J. B. Wang, and J. C. F. Matthews, Efficient quantum walk on a quantum processor, Nat. Commun. **7**, 11511 (2016).

[40] Y.-C. Jeong, C. Di Franco, H.-T. Lim, M. Kim, and Y.-H. Kim, Experimental realization of a delayed-choice quantum walk, Nat. Commun. **4**, 2471 (2013).

[41] D. Xie, T.-S. Deng, T. Xiao, W. Gou, T. Chen, W. Yi, and B. Yan, Topological quantum walks in momentum space with a Bose-Einstein condensate, Phys. Rev. Lett. **124**, 050502 (2020).

[42] S. Dadras, A. Gresch, C. Groiseau, S. Wimberger, and G. S. Summy, Quantum walk in momentum space with a Bose-Einstein condensate, Phys. Rev. Lett. **121**, 070402 (2018).

[43] C. Huerta Alderete, S. Singh, N. H. Nguyen, D. Zhu, R. Balu, C. Monroe, C. M. Chandrashekar, and N. M. Linke, Quantum walks and Dirac cellular automata on a programmable trapped-ion quantum computer, Nat. Commun. **11**, 3720 (2020).

[44] H. Schmitz, R. Matjeschk, C. Schneider, J. Glueckert, M. Enderlein, T. Huber, and T. Schaetz, Quantum walk of a trapped ion in phase space, Phys. Rev. Lett. **103**, 090504 (2009).

[45] F. Zähringer, G. Kirchmair, R. Gerritsma, E. Solano, R. Blatt, and C. F. Roos, Realization of a quantum walk with one and two trapped ions, Phys. Rev. Lett. **104**, 100503 (2010).

[46] P. Xue, B. C. Sanders, and D. Leibfried, Quantum walk on a line for a trapped ion, Phys. Rev. Lett. **103**, 183602 (2009).

[47] P. K. Pathak and G. S. Agarwal, Quantum random walk of two photons in separable and entangled states, Phys. Rev. A **75**, 032351 (2007).

[48] L. Sansoni, F. Sciarrino, G. Vallone, P. Mataloni, A. Crespi, R. Ramponi, and R. Osellame, Two-particle bosonic-fermionic quantum walk via integrated photonics, Phys. Rev. Lett. **108**, 010502 (2012).

[49] M. Karczewski, R. Pisarczyk, and P. Kurzyński, Genuine multipartite indistinguishability and its detection via the generalized Hong-Ou-Mandel effect, Phys. Rev. A **99**, 042102 (2019).

[50] D. S. Simon, S. Osawa, and A. V. Sergienko, Quantum-clustered two-photon walks, Phys. Rev. A **101**, 032118 (2020).

[51] X. Qiang, Y. Wang, S. Xue, R. Ge, L. Chen, Y. Liu, A. Huang, X. Fu, P. Xu, T. Yi, F. Xu, M. Deng, J. B. Wang, J. D. A. Meinecke, J. C. F. Matthews, X. Cai, X. Yang, and J. Wu, Implementing graph-theoretic quantum algorithms on a silicon photonic quantum walk processor, Sci. Adv. **7**, eabb8375 (2021).

[52] E. Farhi and S. Gutmann, Quantum computation and decision trees, Phys. Rev. A **58**, 915 (1998).

[53] Y. Aharonov, L. Davidovich, and N. Zagury, Quantum random walks, Phys. Rev. A **48**, 1687 (1993).

[54] J. Kempe, Quantum random walks: An introductory overview, Contemp. Phys. **44**, 307 (2003).

[55] R. Ahmad, U. Sajjad, and M. Sajid, One-dimensional quantum walks with a position-dependent coin, Commun. Theor. Phys. **72**, 065101 (2020).

[56] C. Liu and N. Petulante, One-dimensional quantum random walks with two entangled coins, Phys. Rev. A **79**, 032312 (2009).

[57] S. E. Venegas-Andraca, Quantum walks with entangled coins and walkers in superposition, in *Proceedings of the 2018 IEEE Globecom Workshops* (IEEE, New York, 2018), pp. 1–6.

[58] S. E. Venegas-Andraca, J. L. Ball, K. Burnett, and S. Bose, Quantum walks with entangled coins, New J. Phys. **7**, 221 (2005).

[59] M. Annabestani, M. R. Abolhasani, and G. Abal, Asymptotic entanglement in a two-dimensional quantum walk, J. Phys. A: Math. Theor. **43**, 075301 (2010).

[60] E. Roldán, C. Di Franco, F. Silva, and G. J. de Valcárcel, N-dimensional alternate coined quantum walks from a dispersion-relation perspective, Phys. Rev. A **87**, 022336 (2013).

[61] D. Li, J. Zhang, F.-Z. Guo, W. Huang, Q.-Y. Wen, and H. Chen, Discrete-time interacting quantum walks and quantum Hash schemes, Quantum Inf. Process. **12**, 1501 (2013).

[62] C. Alonso-Lobo, M. Martinez-Quesada, M. Hinarejos, G. J. de Valcarcel, and E. Roldan, Two-particle coined-quantum walk with long-range interaction, J. Phys. A: Math. Theor. **51**, 455301 (2018).

[63] P. C. S. Costa, F. de Melo, and R. Portugal, Multiparticle quantum walk with a gaslike interaction, Phys. Rev. A **100**, 042320 (2019).

[64] X. Cai, H. Yang, H.-L. Shi, C. Lee, N. Andrei, and X.-W. Guan, Multiparticle quantum walks and Fisher information in one-dimensional lattices, Phys. Rev. Lett. **127**, 100406 (2021).

[65] L. K. Grover, A fast quantum mechanical algorithm for database search, in *Proceedings of the Twenty-Eighth Annual ACM Symposium on Theory of Computing (STOC '96)* (ACM Press, Philadelphia, 1996), pp. 212–219.

[66] L. K. Grover, Quantum mechanics helps in searching for a needle in a haystack, Phys. Rev. Lett. **79**, 325 (1997).

[67] H. Krovi and T. A. Brun, Quantum walks with infinite hitting times, Phys. Rev. A **74**, 042334 (2006).

[68] H. Krovi and T. A. Brun, Hitting time for quantum walks on the hypercube, Phys. Rev. A **73**, 032341 (2006).

[69] P. Prabhu and T. A. Brun, Influence of coin symmetry on infinite hitting times in quantum walks, Phys. Rev. A **105**, 032206 (2022).

[70] A. C. Orthey and R. M. Angelo, Nonlocality, quantum correlations, and violations of classical realism in the dynamics of two noninteracting quantum walkers, Phys. Rev. A **100**, 042110 (2019).

[71] G. Abal, R. Siri, A. Romanelli, and R. Donangelo, Quantum walk on the line: Entanglement and nonlocal initial conditions, Phys. Rev. A **73**, 042302 (2006).

[72] S. K. Goyal and C. M. Chandrashekar, Spatial entanglement using a quantum walk on a many-body system, J. Phys. A: Math. Theor. **43**, 235303 (2010).

[73] A. Vallejo, A. Romanelli, R. Donangelo, and R. Portugal, Entropy production in the quantum walk, Phys. Rev. A **99**, 032319 (2019).

[74] B. Tregenna, W. Flanagan, R. Maile, and V. Kendon, Controlling discrete quantum walks: Coins and initial states, New J. Phys. **5**, 83 (2003).

[75] T. A. Brun, H. A. Carteret, and A. Ambainis, Quantum random walks with decoherent coins, Phys. Rev. A **67**, 032304 (2003).

[76] P. L. Knight, E. Roldán, and J. E. Sipe, Propagating quantum walks: The origin of interference structures, J. Mod. Opt. **51**, 1761 (2004).

[77] Y. Omar, N. Paunkovic, L. Sheridan, and S. Bose, Quantum walk on a line with two entangled particles, Phys. Rev. A **74**, 042304 (2006).

[78] C. M. Chandrashekar and T. Busch, Quantum walk on distinguishable non-interacting many-particles and indistinguishable two-particle, Quantum Inf. Process. **11**, 1287 (2012).

[79] A. Ambainis, E. Bach, A. Nayak, A. Vishwanath, and J. Watrous, One-dimensional quantum walks, in *Proceedings of the Thirty-Third Annual ACM Symposium on Theory of Computing (STOC '01)* (ACM Press, New York, 2001), pp. 37–49.

[80] N. Bleistein and R. A. Handelsman, *Asymptotic Expansions of Integrals*, revised ed. (Dover, New York, 2010).